THE ROLE OF INNER RETINAL INHIBITORY CIRCUITS IN TUNING OFF RETINAL GANGLION CELL OUTPUT

By

Ilya Buldyrev

A DISSERTATION

Presented to the Neuroscience Graduate Program
and the Oregon Health and Science University
School of Medicine
in partial fulfilment of the requirements for the degree of

Doctor of Philosophy

August 2010

School of Medicine

Oregon Health & Science University

CERTIFICATE OF APPROVAL

This is to certify that the Ph.D. dissertation of

ILYA BULDYREV

has been approved

Advisor, W. Rowland Taylor, PhD

Member and Chair, Laurence Trussell, PhD

Member, Matthew Frerking, PhD

Member, Henrique von Gersdorff, PhD

Member, John Williams, PhD

TABLE OF CONTENTS

Acknowledgements

First and foremost I would like to thank my advisor, Dr. W. Rowland Taylor, for providing me with many years of support and instruction in performing this research project, including instruction on all the electrophysiological techniques described in this dissertation. He provided the software for generating light stimuli, and wrote the software for analysing retinal ganglion cell responses. He also engaged with me in many hours of thoughtful discussion on experimental design, interpretation of the results, and helped edit the manuscript. I am also indebted to all members of Dr. Taylor's research group with whom I have crossed paths for providing a very warm and positive environment, especially during difficult times. In particular, I would like to thank Dr. Taylor's former graduate student, Dr. Nicholas Oesch, who introduced me to a lot of the techniques that I continued to use throughout my training, Jacqueline Gayet for her help with all staining protocols and reagents, as well as Dr. Teresa Puthussery and Dr. Sowmya Venkatramani, postdocs in the lab who provided me with a lot of excellent feedback on my results and writing. I would also like to acknowledge Ben Sivyer, Dr. David Vaney's graduate student and close collaborator of Dr. Taylor for commenting on the manuscript and discussing my work with me.

This would not have been possible without the support of my family: my grandmother Anna, a physician and researcher, who inspired me to go into biomedical research, my wife Lavinia who was always there for me, my parents and brother. A special thank you goes to my daughter Andrea for being a constant source of joy.

Abstract

Action potentials in distinct classes of retinal ganglion cell (RGC) encode salient features in the visual environment. While the firing properties of many RGCs are well described, much less is known about the underlying synaptic mechanisms. NMDA receptor mediated excitation of RGCs has been reported, but the physiological significance remains unclear. Here we examine light-evoked synaptic inputs to the center receptive field of OFF brisk-sustained (OFF-BS) RGCs in the rabbit retina and determine the roles of NMDA, non-NMDA and inhibitory inputs in generating the spike output. We confirm that the excitatory inputs to these neurons are mediated by both NMDA and AMPA inputs. The analysis indicates that the NMDA and AMPA receptors are segregated to different synapses, which was evident from a slower rate of contrast adaptation for the NMDA inputs relative to AMPA inputs, and differential effects when GABAergic transmission was blocked - the NMDA inputs were suppressed, while AMPA inputs were enhanced. Moreover, NMDA antagonists blocked relatively more of the action potentials, and excitatory conductance at low than at high contrasts. OFF-BS cells also receive a dis-inhibitory glycinergic input driven by the ON pathway, which enhances contrast-sensitivity at high temporal frequencies, but produces little effect at low temporal frequencies. Thus, we demonstrate two novel retinal circuits that regulate contrast and temporal frequency sensitivity of a specific retinal ganglion cell type. The first relies on separate, NMDA receptor-containing synapses to enhance sensitivity to low contrasts, whereas the second uses a phase-reversed inhibitory input to maintain contrast-sensitivity at high temporal frequencies.

Chapter 1

Introduction

One of the fundamental questions in the study of the nervous system is how it translates external stimuli into signals that brain circuitry can interpret and use to generate responses. There are several difficulties in setting up experiments in the central nervous system that would provide unambiguous answers. One of the foremost is devising a physiologically relevant stimulus for an isolated piece of neural circuitry. An additional problem stems from the complexity of the connections in the brain. Although many brain regions, such as the cerebellum and the hippocampus, display very stereotyped circuit architecture, they exchange information between multiple sensory modalities and from many other parts of the brain. This makes it difficult to determine how they encode specific information.

The visual system holds some advantages in these areas and has long been employed to address questions of how the nervous system processes and transmits information. This is due to its well-categorized neuronal populations, the appearance of orderly circuitry, even up to the cortical level, and the ease of manipulating visual stimuli. The retina, in particular, is an attractive experimental model, because it is a complete central nervous system circuit, which processes a natural stimulus, light inputs received by photoreceptors, without some of the additional complexity produced by interconnections in the brain. The experimental approach described here takes advantage of intact retinal circuitry to examine how visual information gathered by photoreceptors is routed through several types of excitatory and inhibitory interneurons to recombine in

retinal ganglion cells (RGCs), the output neurons of the retina. This dissertation focuses on a particular type of RGC, known as the OFF brisk sustained (BS) in the rabbit retina. This cell-type has a small receptive field and a particular response profile that is unlike some of the other, primarily larger RGC types, which have been studied in greater detail. My findings describe the types of light stimulus-evoked inputs that this cell receives under daylight conditions. The goal is to discern what type of information these inputs carry regarding the stimulus. The results presented here are interesting in light of studies that have been done on inputs to other RGC types, because even though similar types of interneurons play a role in generating receptive fields of different RGCs, the information that is transmitted is not always the same.

Chapter 2 of this dissertation presents the findings regarding light-evoked excitatory inputs to OFF BS RGCs. These consist of an AMPA/Kainate receptor-mediated component, and an NMDA receptor-mediated component. The relative contribution of these two components to the spike output of the RGC changes with stimulus strength, and the involvement of inhibition in regulating these excitatory inputs is assessed.

Chapter 3, in turn, focuses on the inhibitory inputs that OFF BS RGCs receive. The inhibition in these neurons has the polar opposite response to changes in light intensity compared to the excitatory inputs. Thus, the primary, light-evoked inhibition in these OFF RGCs acts in concert with excitation to increase spiking in the cell. This unusual arrangement has been observed in other OFF RGC types in the retina. However, it may involve different subtypes of amacrine cell interneurons, and convey different information depending on the visual pathway.

Lastly, in chapter 4 I will discuss the relevance of these different types of inputs to encoding temporal and spatial features of the visual environment. I propose some experiments that may uncover the mechanisms by which these inputs might achieve their effects in the RGC.

Bipolar cells initiate parallel processing in the retina

In daylight, the mammalian retina relies on two to three types of cone photoreceptors to encode all the information regarding temporal light intensity changes, and spatial variations in light intensity across the visual field. The photoreceptors differ from each other in the absorbance spectra of their photosensitive opsin pigments, but in mammals other than primates, there is only one type of cone, usually long wavelength sensitive, that predominates. Therefore, a lot of the information that is processed downstream of the photoreceptors under bright illumination originates from one type of photoreceptor and in mammals such as the rabbit is not thought to deal with color vision. Nonetheless, in all the mammalian retinas that have been studied in detail there are at least ten distinct types of bipolar cells, the glutamatergic interneurons that connect photoreceptors to RGCs (Reviewed by Wassle, 2004). Bipolar cells have been classified into two primary types based on the level of their axon terminal branching in the inner plexiform layer (IPL) of the retina (Famiglietti and Kolb, 1976; Bloomfield and Miller, 1986) and their response to light, depolarizing or hyperpolarizing (Kaneko, 1970; Dacheux and Miller, 1976). Neurons in the retina that depolarize in response to increases in light intensity have been termed “ON”, and those that hyperpolarize have been termed “OFF”(Hartline, 1938; Werblin and Dowling, 1969). During increases in light intensity,

when photoreceptors are hyperpolarized and slow their release of glutamate, ON bipolar cells are depolarized. ON type bipolar cells express metabotropic, mGluR6, glutamate receptors, which inhibit the cell in the presence of glutamate by gating a cation channel that has recently been identified as the transient receptor potential (TRP) M1 (Nawy and Jahr, 1990; Masu et al., 1995; Morgans et al., 2009; Koike et al., 2010). By contrast, OFF bipolar cells express ionotropic glutamate receptors, such as α-amino-3-hydroxyl-5-methyl-4-isoxazole-propionate (AMPA) and kainate receptors, at their dendrites and are hyperpolarized when glutamate release from cones is decreased (Saito and Kaneko, 1983; Slaughter and Miller, 1983b). The ON and OFF types of bipolar cells have each been divided into approximately five subtypes based on their morphology and gene expression characteristics (Famiglietti and Kolb, 1976; McGuire et al., 1984; MacNeil et al., 2004; Wassle et al., 2009). Differences in how these bipolar cell subtypes filter inputs from photoreceptors have been identified using intracellular recording techniques (Nelson and Kolb, 1983; Awatramani and Slaughter, 2000; DeVries, 2000).

Although the output of photoreceptors appears to be diverted along at least ten specific pathways, no all-encompassing hypothesis has been presented for divergence of photoreceptor signals into parallel pathways. Splitting an input among multiple channels introduces noise into the system, making it harder for the brain to detect weak stimuli. In order to counteract this, the retina employs a substantial amount of tightly regulated coupling among photoreceptors, inhibitory interneurons (horizontal and amacrine cells), as well as specific bipolar and ganglion cell types (Kaneko, 1971; Zhang and Wu, 2009). Bipolar cells and ganglion cells employ coupling and large receptive fields among inhibitory interneurons to form a center-surround antagonism, averaging the mean noise

over broad spatial areas and subtracting it from a narrow region of interest in the center of a neuron's receptive field (Baylor et al., 1971; Thibos and Werblin, 1978; Srinivasan et al., 1982; Burkhardt et al., 1988; Cook and McReynolds, 1998; Taylor, 1999; Flores-Herr et al., 2001; McMahon et al., 2004; Ichinose and Lukasiewicz, 2005) Canceling noise in temporal and spatial scales allows the retina to encode weak signals, counteracting the noise introduced by transmitting information over multiple analog synapses (Borghuis et al., 2009). Additionally, inputs from multiple photoreceptors converge on single bipolar cells to amplify the signal under low-light conditions, and in the peripheral retina, where spatial resolution can be compromised (Sterling et al., 1988).

In spite of the evidence for convergence and its benefits for improving the signal to noise ratio in the retina (Demb et al., 2004), electron microscopy reconstruction studies have conclusively demonstrated the divergence of output from photoreceptors. In the cat, single cone photoreceptors split their output among multiple bipolar cells (Cohen and Sterling, 1990), and in the primate fovea two or three midget ganglion cells receive the output of a single long or medium wavelength-sensitive cone (Wassle et al., 1989). What is the role of signal divergence in the retina? Parallel pathways of signal transmission may be necessary for RGCs to efficiently encode the full dynamic range of photoreceptor output. Consider that if the ON and OFF pathways were combined into one, RGCs would be required to signal decreases in light intensity as decreases in firing rate and increases in light intensity as increases in firing rate. In order to do so faithfully, RGCs would have to maintain very high firing rates, possibly over 100 Hz, in the absence of any changes in light intensity. This would be energetically costly, and introduce ambiguity, because in order for a cortical circuit to quickly respond a dark stimulus, it would have to recognize

a decrease in activity with the same temporal precision as it does a burst of spikes. With both an ON and an OFF pathway, the beginning and end of any type of visual stimulus are encoded as bursts of activity. Further subdivision of the ON and OFF pathways is based on how particular types of bipolar cells and RGCs transduce signals in order to emphasize particular temporal or spatial features in the visual environment.

Retinal ganglion cell output comprises multiple channels for visual information

Signal processing in the retina culminates in RGCs, which encode the graded output of neurons that feed into them as trains of action potentials. Like the bipolar cells, which can be distinguished based on the depth of axon terminal termination, RGCs can be classified based on stratification level of their dendrites in the IPL, and include ON and OFF subtypes. The axons of different RGC types represent separate pathways for visual information to the dorsal lateral geniculate nucleus and other brain regions. Unlike bipolar cells, however, which are exclusively ON or OFF and generally have similar receptive field dimensions, RGC subtypes include cells that respond to both light intensity increases and decreases (ON-OFF cells) and cell types that vary dramatically in the spatial extent over which they collect their inputs (Barlow, 1953; Kuffler, 1953). Some RGC types encode more complex spatio-temporal features of the stimulus, such as moving edges, stimulus orientation and direction of motion (Levick, 1967; Oyster and Barlow, 1967}. Thus, the simple center-surround antagonism found in the receptive fields of bipolar cells is transformed by amacrine cells in the inner retina into the more complex receptive fields of RGCs (Fried et al., 2002; Taylor and Vaney, 2002; van Wyk et al., 2006; Russell and Werblin, 2010; Sivyer et al., 2010).

More than ten types of RGCs have been identified morphologically in the rabbit and other mammalian retinas. Each type is expected to tile the retinal surface, and thus transmit a full representation of the visual field as a separate channel to the brain. The diversity of RGC response characteristics first became apparent during recordings of spiking responses of individual RGCs to focal stimuli (stimuli focused within the receptive field of a particular light responsive neural unit) in the retina of the frog (Barlow, 1953), cat (Kuffler, 1953), monkey (Hubel and Wiesel, 1960), and rabbit (Barlow and Hill, 1963). In the cat, the ON and OFF units were subdivided into cells that had brisk or sluggish axon conductance velocities, and exhibited transient, sustained or sluggish responses to focal stimuli (Enroth-Cugell and Robson, 1966). RGCs identified in the rabbit retina included those that responded to edges within their receptive field, local edge detectors (LEDs), cells that were inhibited by objects in their receptive fields, uniformity detectors, as well as orientation selective and direction selective units (Barlow and Levick, 1965; Levick, 1967). In the cat, RGCs with brisk sustained responses were termed X cells, and those with brisk transient responses were termed Y cells (Enroth-Cugell and Robson, 1966). One of the primary differences between these two cell types is how they sum inputs in the spatial domain (Hochstein and Shapley, 1976b; Shapley and Victor, 1978). X cells were found to sum linearly, meaning that if light intensity is dimmed over exactly half of the X-cell receptive field, and brightened over the other half, the two inputs cancel each other, and the cell does not respond. Y cells, on the other hand were defined as RGCs that sum their inputs nonlinearly, giving more power to the preferred stimulus, light intensity increases or decreases depending on whether the cell being recorded is ON or OFF. Y and X type cells in the cat were linked to morphological

subtypes of RGCs termed α and β respectively (Boycott and Wassle, 1974; Peichl and Wassle, 1979). Alpha RGCs were shown to have larger dendritic fields than β RGCs at the same retinal eccentricities (Linsenmeier et al., 1982). Testing spatial summation of Y cells with gratings of different spatial frequencies allowed early investigators to make predictions about the origin of nonlinear summation in Y cells before intracellular recordings were possible. These experiments showed that nonlinear spatial summation occurs on small scales, and arises from spatial subunits with rectified responses that are much smaller than the entire RGC receptive field (Hochstein and Shapley, 1976a). More recently, intracellular recordings from Y-type RGCs in the guinea pig retina showed that the rectified subunits within the Y RGC receptive field are comprised of excitatory inputs from individual bipolar cells (Demb et al., 2001a; Crook et al., 2008b). Their nonlinear summation properties are independent of GABAergic or glycinergic inhibition in the IPL (Demb et al., 2001b). Thus, the unique spatio-temporal characteristics of the Y-cell channel, which has been traced up to the level of the dorsal lateral geniculate nucleus in the brain (Shapley and Hochstein, 1975), are generated by the intrinsic properties of specific bipolar cells.

The simplest model of parallel processing in the retina would assume that linear spatial summation in an X-type RGC would arise from bipolar cells that sum cone inputs linearly, just as Y-type RGCs receive inputs from non-linear bipolar cells. As previously mentioned, individual bipolar cell subtypes within the ON and OFF categories possess unique temporal response properties to glutamate release from cones. OFF bipolar cells differ in their complement of dendritic AMPA and kainate receptors, which seems to correspond to whether they respond to light modulations or glutamate application with a

large transient or a smaller, but sustained modulation of their membrane potential (DeVries, 2000). Likewise, ON bipolar cells have transient and sustained varieties (Awatramani and Slaughter, 2000; Euler and Masland, 2000). Presumably the linear bipolar cells that provide inputs to X-type RGCs would be the ones that lack a fast transient response to a flashed spot. However, in the cat retina the linear X RGCs have been shown using serial electron micrograph reconstructions to receive inputs from multiple bipolar cell types, some of which have transient light responses (Sterling et al., 1988; Nelson et al., 1993). This prevents any simplistic view of how RGC receptive field properties are generated. The presence of linear X RGCs in the retina may require additional neural circuitry, considering that the output of some many bipolar cells is rectified, particularly in the OFF pathway, and that multiple bipolar cell types combine to provide input to single RGCs (Kim and Rieke, 2001; Chichilnisky and Kalmar, 2002; Zaghloul et al., 2003). There has not been a characterization of spatial summation properties among bipolar cell types, or a systematic study of which particular bipolar cell types provide input to specific RGCs.

A complicating factor in delineating processing pathways in the retina has been the difficulty of isolating the morphological correlates of X and Y physiological RGC types. While RGCs with α or β type morphology have been distinguished in the retinas of all the mammalian species, physiological properties of many RGC types have not been matched to morphology even within the retina of a single species (Rockhill et al., 2002). In the rabbit, for example, the X and Y designations were not found useful in classifying RGCs, because most RGCs have low maintained firing rates *in vitro*, and have highly non-linear responses (Caldwell and Daw, 1978; Vaney et al., 1981a; Amthor et al.,

1989b). Moreover, in the primate retina, the debate over whether the parasol/ magnocellular pathway corresponds to the Y pathway of other mammals has been ongoing. Initial studies indicated that the macaque retina had both X and Y physiological RGC types (de Monasterio, 1978), however whether these types corresponded to the parvocellular and magnocellular pathways respectively was soon called into question (Kaplan and Shapley, 1982). Recent studies recording from the macaque retina *in vitro* indicate that there are two distinct α-like morphological RGC types that have Y-cell physiology (Crook et al., 2008a; Crook et al., 2008b). Like the Y cells in the cat and guinea pig, these neurons have linear spatial summation that predominates at low spatial frequencies, and a non-linear frequency-doubled response that remains strong at high spatial frequencies and likely originates from an array of rectified bipolar cell inputs (Demb et al., 2001b; Crook et al., 2008b). The appearance of linear or non-linear spatial summation may depend on the spatial frequency of stimulus used to probe the receptive field, and other experimental conditions, such as whether the stimulus is applied *in vivo* through the lens of the eye of an anesthetized animal, or projected *in vitro* onto a flat-mount retinal preparation. Fine gratings may be blurred when indirectly projected onto the retina in live animals, thereby decreasing the nonlinear component of the response, which is larger at high spatial frequencies.

Amacrine cells exchange signals between the ON and OFF channels

The broad picture that has emerged over decades of recording the spike output of RGCs and the dorsal lateral geniculate nucleus neurons to which they project is that retinal circuitry contains diverse mechanisms of filtering visual information. Measuring

the output of both the X and Y pathways demonstrated varying degrees of gain control among cell types with signal transduction being affected differently depending on contrast and temporal frequency (Shapley and Victor, 1978; Victor, 1987). Victor and Shapley proposed that contrast gain control and nonlinear spatial summation, both prominent in Y cells, were a result of selective inhibitory input from amacrine cells, but without intracellular recordings it was impossible to pin down which elements of retinal circuitry were actually responsible. While the likely source of the non-linear behavior seen in Y cells was later attributed to the intrinsic properties of cone bipolar cells (Demb et al., 2001b; Beaudoin et al., 2008), the role of feed-forward and feedback inhibition generated by amacrine cells in the IPL in shaping RGC receptive field dynamics remains a source of debate.

Only three of the several dozen morphological types of amacrine cells have been definitively implicated in specific pathways of visual processing in the retina. The AII amacrine cell receives input from rod bipolar cells, providing a conduit for rod photoreceptor output to the cone pathway under low light conditions (Kolb and Famiglietti, 1974; Dacheux and Raviola, 1986). The A17 type (termed S1 and S2 in the rabbit) provides feedback inhibition to rod bipolar cells (Nelson and Kolb, 1985; Dacheux and Raviola, 1986; Vaney, 1986; Grimes et al., 2010), while cholinergic starburst amacrine cells have been implicated in generating direction selectivity of the four subtypes of direction selective RGCs (Vaney et al., 1981b; Euler et al., 2002; Taylor and Vaney, 2002). The functions of other amacrine cell types remain unknown. Amacrine cells vary in their dendritic field size, intrinsic physiological properties, connectivity across laminae of the IPL, electrical coupling with bipolar cells and other amacrine cells,

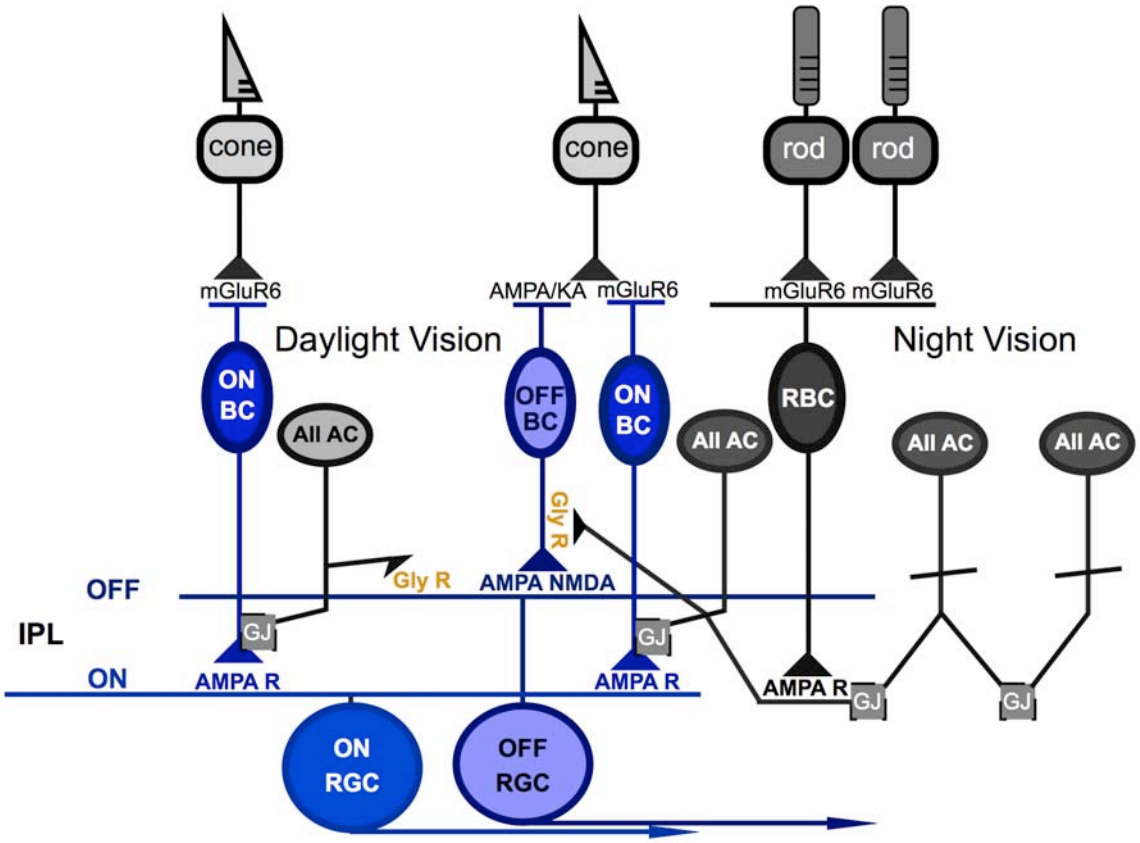

Figure 1.1 Dual function AII amacrine cells mediate night and daylight vision.

Diagram showing the functional connectivity of the AII amacrine cell under light-adapted conditions when rod photoreceptor responses are saturated (left), and under dim illumination when only the rods are active (right).

When part of the rod pathway (right), AII amacrine cells get a glutamatergic input from rod bipolar cells, and make a sign-conserving electrical connection with ON bipolar cells, and a sign-inversing, inhibitory glycinergic synapse onto OFF bipolar cell terminals. Under dim illumination AII amacrine cells are extensively coupled to other amacrine cells via connexin 36 gap junctions.

Bright illumination (left) leads to the uncoupling of AII amacrine cells. AII amacrine cells now provide a feedforward inhibitory connection from ON bipolar cells to OFF RGCs.

and neurotransmitter content. Their staggering diversity suggests multiple roles in processing information, and makes it possible that specific amacrine cell types may subserve distinct visual information channels that emerge from the retina.

One of the goals of the work presented in this dissertation is to determine the role of amacrine cell inhibition in shaping OFF BS RGC receptive field properties, and contrast that to what has been shown for inhibition in other types of RGCs. Whole-cell

voltage-clamp recordings from the whole-mount *in vitro* retinal preparation are allowing for a detailed analysis of the excitatory and inhibitory inputs to RGCs. These techniques have greatly aided the classification of RGCs based on physiological properties, and the assigning of specific functions to elements of retinal circuitry, something that has been difficult using solely extracellular RGC responses. Moreover, filling RGCs, and amacrine cells with fluorescent dyes during recordings is proving useful in matching the physiological receptive field properties to the morphological characteristics of different neuronal classes.

Using the above-mentioned techniques several recent studies have identified a novel role for the AII amacrine cell, which was previously only known for transducing rod signals (Manookin et al., 2008; Munch et al., 2009). AII amacrine cells have broad dendritic stratification in the IPL, making contacts with ON and OFF cone bipolar cells, and are electrically coupled to each other and to ON cone bipolar cells via ion-permeable gap junctions composed of connexin 36 molecules (Cohen and Sterling, 1986; Vaney et al., 1991; Strettoi et al., 1992; Xin and Bloomfield, 1997). They receive excitatory glutamatergic inputs from rod bipolar cells (Raviola and Dacheux, 1987), and release glycine at synaptic contacts with OFF bipolar cell terminals and OFF RGCs (Muller et al., 1988). Under low-light, rod-dominant conditions an AII amacrine cell is depolarized by focal increases in light intensity due to the excitatory input that it receives from the depolarizing rod bipolar cells (See review by Bloomfield and Dacheux, 2001). The depolarization is transmitted to ON cone bipolar cells via gap junctions causing an activation of the ON pathway (Deans et al., 2002; Veruki and Hartveit, 2002; Bloomfield and Volgyi, 2004). The same depolarization of the AII inhibits the OFF pathway as these

amacrine cells release glycine onto OFF bipolar cell terminals and directly onto OFF RGC dendrites (Muller et al., 1988; Munch et al., 2009).

The more recently discovered function of AII amacrine cells relates to their function under daylight conditions when rod responses are saturated. When light-adapted, the AII transmits a crossover feed-forward inhibitory signal from the ON to the OFF pathway (Manookin et al., 2008; Munch et al., 2009; van Wyk et al., 2009). Gap junctions between ON cone bipolar cells and AII amacrine cells function in reverse by transmitting light-evoked ON cone bipolar membrane potential changes to the AII, (Xin and Bloomfield, 1999; Pang et al., 2007; Veruki and Hartveit, 2009) which serves to inhibit or disinhibit the OFF pathway through glycinergic synapses (Manookin et al., 2008). Manookin et al., (2008) demonstrated that under dark background illumination ON α RGC responses to a focal step change in light intensity were reduced by bath application of connexin 36-selective gap junction blocker quinine (Srinivas et al., 2001), while they were insensitive to quinine when the same stimulus was presented on a bright background. Consequently, they showed that either quinine, the ON pathway blocker L-AP4, or strychnine, which blocks glycine receptors could be used to block light-evoked inhibitory inputs to OFF α RGCs. This inhibitory input to OFF RGCs was insensitive to AMPA and NMDA glutamate receptor antagonists CNQX and D-AP5. The putative role of AII amacrine cells as mediators of crossover inhibition from ON cone bipolar cells to the OFF pathway was confirmed by the strong reduction of light-evoked glycinergic inhibition in OFF-sustained RGCs of connexin 36 knockout mice under light-adapted conditions (van Wyk et al., 2009).

A possible function for the ON to OFF channel crossover inhibition mediated by AII amacrine cells is that it could enhance spiking in OFF RGC in response to darkening stimuli. During focal decreases in light intensity, the inhibitory input to OFF RGCs decreased below its tonic level under steady illumination. This was particularly prominent in guinea-pig OFF δ cells (Manookin et al., 2008) and mouse OFF-sustained cells (van Wyk et al., 2009), and is proposed to contribute to the OFF cell's spike output by increasing its membrane resistance and decreasing the hyperpolarizing drive. Thus, feedforward crossover inhibition in OFF RGCs may act in concert with excitation from OFF bipolar cells to drive spiking. Conversely, increases in inhibitory input to OFF RGCs during positive light steps, could suppress spiking in cells that maintain a firing rate under steady background illumination. Before intracellular recordings of light-evoked synaptic inputs to RGCs were possible, one group of investigators pharmacologically induced changes in spike rates of cat OFF RGCs by blocking synaptic transmission in the ON channel with APB (Wassle et al., 1986). Wassle et al. were able to modulate OFF brisk-sustained and brisk-transient RGC firing rates by local, pulsatile application of APB, and this modulation was inhibited by coapplication of strychnine. Thus, the ability of the ON channel to affect activity in OFF RGCs through an inhibitory connection has been established. However, the contribution of ON channel-driven inhibition to signal transduction in the OFF channel has not been systematically tested among different RGC types, and the mechanisms by which crossover inhibition may affect spiking in OFF RGCs are not yet understood.

The results in chapter 3 demonstrate the contribution of ON channel-driven inhibition to OFF BS RGC spike output. Crossover inhibition enhances the transient

component of light responses, contributes to their contrast adaptation at high temporal frequencies, and linearizes responses over a range of temporal contrast. These results demonstrate specific roles of crossover inhibition in a single retinal pathway, one with high spatial resolution and relatively high temporal frequency sensitivity. So far only a few studies have examined the effect of crossover inhibition on OFF RGC spike output (Molnar et al., 2009; Munch et al., 2009). Other authors who have examined crossover inhibitory currents showed considerable differences in their temporal properties among different types of RGCs (Manookin et al., 2008; van Wyk et al., 2009). The amount of inhibitory current shut off by a darkening stimulus (disinhibition) varied between the cat OFF α and δ RGC responses shown in the study by Manookin et al. In mouse RGCs, crossover inhibition appeared much more transient in OFF transient A-type cells than in the sustained variety, and similarly to the cat, the sustained cells appeared to have much more disinhibition in response to darkening stimuli (van Wyk et al., 2009). Differences in the tonic inhibitory input and the temporal features of the crossover input suggest that distinct spatio-temporal visual pathways in the retina may employ crossover inhibition for different purposes, and that it may be mediated by diverse amacrine cells.

Based on intracellular recordings of bipolar, amacrine cells and RGCs, Molnar et al. (2009) presented a theoretical model that showed how crossover inhibition could generate linear spatial summation in an RGC when the excitatory inputs to the cell are nonlinear. In confirmation, they demonstrated disruption of linear spatial summation in OFF RGCs of unknown type and morphology by blocking the ON channel contribution using APB. Another study of the contribution of crossover inhibition to spatial summation arrived at a similar conclusion (Munch et al., 2009). These authors

demonstrated that a specific type of mouse OFF RGCs displays a preference for "approaching" stimuli, dark bars that widen in the receptive field. This preference was abolished by blocking the ON pathway with L-AP4. Munch et al. (2009) showed that during other types of motion, where both bright and dark bars were traversing the receptive field, the crossover inhibitory input inhibited both the RGC directly and presynaptically at the OFF bipolar cell terminals.

The results presented here do not examine how crossover inhibition affects spatial summation, and a prediction of whether the model proposed by Molnar et al. would hold for OFF BS RGCs is difficult due unknown factors, such as which type of amacrine cells mediates crossover inhibition to OFF BS RGCs and how spatial summation occurs in the amacrine cells themselves. Spatial summation in AII amacrine cells, the putative mediators of crossover inhibition, has not been studied extensively (Bloomfield, 1992). Interpretation of experimental results regarding spatial properties of AII receptive fields are susceptible to error, because amacrine cell recordings are typically done in a retinal slice preparation, where portions of the receptive field are severed. Moreover, intracellular recordings may be affected by the extensive electrical coupling of AII amacrine cells to other AIIs, which is regulated by dopaminergic activation of cyclic AMP synthesis, and can dramatically alter receptive field size and properties (Hampson et al., 1992; Mills and Massey, 1995; Xia and Mills, 2004). The state of retinal light adaptation affects coupling among AII amacrine cells through the dopaminergic input (Bloomfield et al., 1997). Hence, the contribution of crossover input to RGC linear spatial summation *in vivo* could be different at mesopic and photopic light levels. At mesopic light levels, when amacrine cells may maintain some coupling and sum inputs

over a wider area (Bloomfield and Volgyi, 2004), an AII receptive field may have the same or larger spatial extent than the RGC to which it provides an input, particularly for small RGCs. Thus at lower ambient light levels, an AII may increase its spatial resolution relative to the bipolar cell input that an RGC receives, and would only contribute information regarding temporal contrast. The possibility of light adaptation influencing the spatio-temporal properties of crossover inhibition will need to be addressed in future experiments.

The hypothesis that crossover inhibition linearizes OFF RGC responses is challenged by a study showing that crossover inhibition can tonically inhibit OFF bipolar cell terminals presynaptic to the RGC (Liang and Freed, 2010). In the case of the G5 and LED RGCs in the rabbit, blocking the ON pathway increases the amount of tonic excitatory input. As a result, the excitatory inputs become less rectified, acquiring the ability to signal increases in light intensity as well as decreases. Thus, blocking ON crossover inhibition-mediated rectifying input would allow more linear spatial summation in OFF RGCs, which contradicts the aforementioned hypothesis that crossover inhibition itself linearizes spatial summation (Molnar et al., 2009). The presynaptic rectifying inhibition described by Liang and Freed, like the direct ON channel-driven inhibitory input to RGCs, is dependent on glycinergic inhibition, which suggests that it is mediated by a narrow-field amacrine cell (Liang and Freed, 2010). Our lab, however, did not observe a decrease in tonic excitatory input to rabbit orientation selective and OFF BS RGCs as a result of blocking the ON pathway (Venkatramani, Taylor, Unpublished data and Figure 3.3). The conflicting findings regarding the role crossover inhibition and its action at pre versus postsynaptic sites suggest that it could be

mediated by different amacrine cell types depending on the class of bipolar cell or OFF RGC being recorded.

The role of narrow-field amacrine cells other than the AII in shaping the spatiotemporal properties of RGC receptive fields remains unclear. Some amacrine cells in the cat, rat and rabbit have been observed with Golgi staining and other methods to have very similar morphology to the AII (Kolb et al., 1981; Menger et al., 1998; MacNeil et al., 1999). In the rabbit approximately 9 narrow-field bistratified or diffusely stratified amacrine cell types have been identified (1999; MacNeil et al., 1999, Figure 1.2). Similarly, an investigation of glycinergic amacrine cells in the rat retina yielded 8 types of amacrine cells immunoreactive for glycine transporter 1, all of which have small dendritic fields, and dendrites that ramify in both the ON and OFF sublamina of the IPL (Menger et al., 1998). In the cat, one such cell, termed A8, receives much fewer synaptic inputs from rod bipolar cells and more contacts from ON and OFF cone bipolar cells than the AII, and unlike the AII hyperpolarizes to focal light stimulation (Kolb and Nelson, 1996). This cell type could mediate inhibition crossing from the OFF to the ON pathway. This reverse crossover has recently been documented in rabbit ON-beta RGCs (Chen et al., 2010). Other glycinergic amacrine cells may have inhibitory feedback and feedforward functions within the ON and OFF channels (Eggers and Lukasiewicz, 2006; Chavez and Diamond, 2008), or serve to inhibit GABAergic amacrine inputs, which provide lateral inhibition to RGCs in the IPL (Russell and Werblin, 2010). Contributing to this evidence, results presented here in chapter 3 indicate that glycinergic inhibition regulates GABAergic inputs to OFF BS RGCs. The functional role of amacrine to RGC and amacrine on amacrine cell inhibition (Eggers and Lukasiewicz, 2010) is only

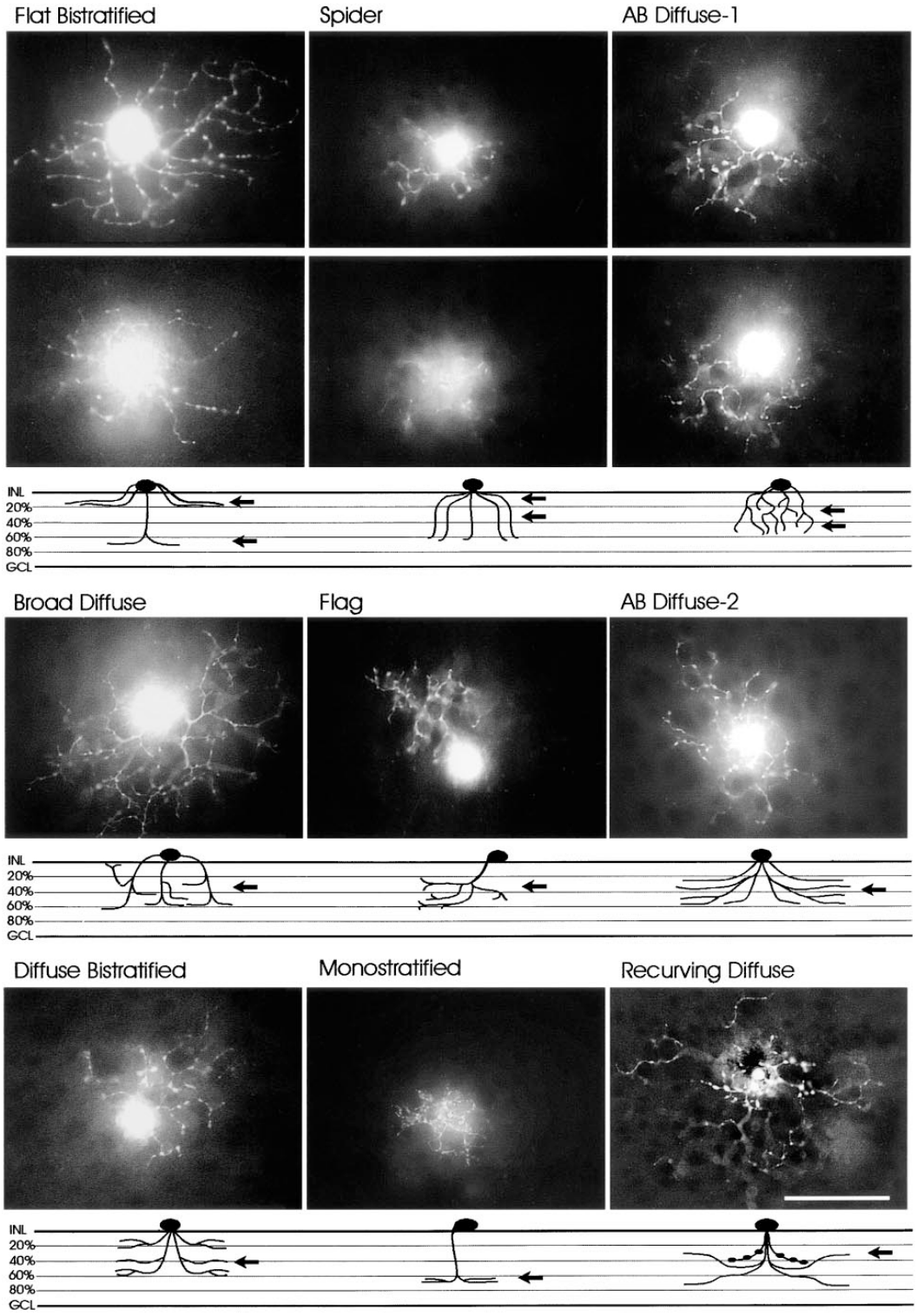

Figure 1.2 Narrow-field amacrine cells of the rabbit retina.
Taken from **Figure 4, MacNeil and Masland, 1998, Neuron.**
INL = inner nuclear layer, GCL = ganglion cell layer. Black arrows indicate the inner plexiform layer level at which the above photomicrographs were taken. Masland and MacNeil visualized cells with fluorescent rhodamine 123 injections.

beginning to be addressed, and will be the focus of much of the future research on retinal physiology (see review by Lukasiewicz, 2005).

Postsynaptic signal processing by retinal ganglion cells: focus on NMDA receptors

Much of this literature review, and the majority of retinal physiologists have focused on the circuitry preceding RGCs. Only recently has there been more investigation of intrinsic physiological properties of RGCs and how they contribute to the unique spatiotemporal properties of the signaling pathways that emerge from the retina. Since the early days of retinal research, anatomical studies have provided insight into the diversity of RGCs. The most obvious anatomical characteristics by which RGC types can be distinguished are the area covered by the dendrites, the level that dendrites stratify in the IPL, and the dendritic branching pattern. On the basis of these traits anatomists have predicted the existence of a dozen or more types of RGC in the mammalian retina (Amthor et al., 1989b; 1989a; Rockhill et al., 2002; Famiglietti, 2004; Famiglietti, 2005). The dendritic field area, which somewhat closely corresponds to the receptive field area of a particular RGC, indicates whether it functions in a high or low spatial acuity pathway. An RGC's dendritic ramification, either in the a or b sublamina of the IPL, or both, determines whether it gets input from OFF, ON or both types of bipolar cells. However, the role of other anatomical features, such as dendritic density, symmetry and branching pattern is still a matter of speculation.

From the functional perspective distinctions among RGCs can be drawn based on specific patterns of neurotransmitter receptor and voltage gated ion channel expression. Specifically, differences in NMDA receptor expression and contribution to excitatory inputs have recently been observed among different RGCs (Zhang and Diamond, 2009;

Manookin et al., 2010). Although many NMDA receptors are blocked by Mg^{2+} at typical RGC resting membrane potentials, initial studies showed that NMDA receptors make a small but significant contribution to light-evoked spike output of RGCs (Slaughter and Miller, 1983a; Lukasiewicz and McReynolds, 1985; Massey and Miller, 1990; Cohen and Miller, 1994). However, several other investigations did not reveal NMDA receptor contribution to light-evoked responses (Coleman and Miller, 1988; Kay and Ikeda, 1989). Although these early findings were contradictory, NMDA receptor contribution to RGC excitatory inputs were seen by researchers doing intracellular recordings (Mittman et al., 1990; Cohen et al., 1994; Zhou et al., 1994; Cohen, 1998). However, NMDA receptors were not observed as a component of spontaneous excitatory postsynaptic currents (sEPSCs) in salamander RGCs (Taylor et al., 1995), which led to the hypothesis and direct observations that NMDA receptors are localized perisynaptically in many RGCs (Matsui et al., 1998; Zhang and Diamond, 2006).

It remains unclear to what extent NMDA receptors are involved in encoding visual stimuli. Since NMDA receptors do not form a large part of light-evoked excitation in RGCs and became best known for their role in synaptic plasticity, and development, they were not the focus of attention for most investigators studying visual processing in the retina. Nonetheless, NMDA receptors are known to mediate transmission of sensory information in other CNS regions, such as thalamocortical circuits (Miller et al., 1989; Gil and Amitai, 1996; Hull et al., 2009). In the rodent somatosensory barrel cortex, specialized NMDA receptors, which conduct more current at negative membrane potentials due to their subunit composition, contribute to EPSCs in excitatory neurons that get inputs from thalamic sensory afferents, but not in inhibitory interneurons that

receive the same input (Hull et al., 2009). The IPL of the retina is know to express NMDA receptor subunits with lower Mg^{2+} affinity, such as NR2C and NR3, that would allow larger conductances at resting potentials (Brandstatter et al., 1998; Das et al., 1998; Grunder et al., 2000; Wong et al., 2002; Sucher et al., 2003).

Recent evidence suggests NMDA receptors are more active in signal transduction in OFF, but not in ON RGCs (Zhang and Diamond, 2009; Manookin et al., 2010). The first conclusive evidence for differences in NMDA receptor expression between the ON and OFF RGCs emerged from the observation that sEPSCs in OFF RGCs have an NMDA receptor component, but the ones in ON RGCs do not (Sagdullaev et al., 2006). Moreover, an NMDA component in ON RGC EPSCs could be evoked by blocking presynaptic GABAergic inhibition (Sagdullaev et al., 2006). Subsequently it was shown that ON RGCs express primarily NMDA NR2B subunit-containing receptors that localize outside of synaptic zones while OFF RGCs express NMDA NR2A receptors that are colocalized with postsynaptic density proteins. (Kalbaugh et al., 2009; Zhang and Diamond, 2009). In light of the evidence that ON RGC NMDA receptors are perisynatic, a new study suggests that NMDA receptors contribute to light-evoked output of OFF, but not ON α RGCs, even at high stimulus intensities (Manookin et al., 2010).

These differences in NMDA receptor localization and contribution to light response may help explain some of the asymmetry seen in contrast encoding between ON and OFF RGCs (Chichilnisky and Kalmar, 2002; Zaghloul et al., 2003}. However, this would be very difficult to test, because the differences between the ON and OFF channels may arise due to multiple factors, such as circuit connectivity and differences in the intrinsic properties of ON and OFF bipolar cells. An easier comparison may be drawn by

studying different types OFF RGCs that may get input from some of the same bipolar cells, but vary in NMDA receptor expression. Indeed, differences in NMDA receptor contribution to excitatory inputs among two RGCs with OFF responses and large receptive fields have now been observed (Manookin et al., 2010). Additionally, an RGC with a small receptive field, the LED, does not appear to have a significant NMDA receptor component in its light-evoked inputs (van Wyk et al., 2006).

The work presented here focuses on OFF BS RGCs, a different type of small RGC, which is distinguished by a large NMDA receptor input. In the following chapter, I demonstrate how NMDA receptors contribute to its ability to encode visual contrast.

Chapter 2

NMDA receptors enhance temporal contrast sensitivity in OFF brisk-sustained RGCs

Ilya Buldyrev and W. Rowland Taylor

Introduction

NMDA receptors are expressed in RGCs of all the vertebrate species studied, and are known to contribute to light-evoked excitatory conductance and spike output (Slaughter and Miller, 1983a; Lukasiewicz and McReynolds, 1985; Aizenman et al., 1988; Mittman et al., 1990; Cohen et al., 1994; Zhou et al., 1994). However, their role in processing visual information is not well understood. Here, we present evidence that in OFF brisk-sustained (BS) RGCs NDMA receptors contribute to spike output, increasing sensitivity to low temporal contrast stimuli. OFF BS RGCs have some of the smallest dendritic areas among rabbit RGCs and thus form a high acuity pathway to cortical visual centers. BS RGCs may represent a rabbit homologue of the X or β RGCs identified in the cat and other mammals (Enroth-Cugell and Robson, 1966; Victor et al., 1977; Vaney et al., 1981a; Troy, 1983; Pu and Amthor, 1990; Rockhill et al., 2002). Rabbit OFF BS RGC dendrites are morphologically similar to those of another small RGC, the local edge detector cell (LED). However, as their name suggests, OFF BS RGC temporal response properties are much faster than the relatively sluggish LEDs (van Wyk et al., 2006). This may be attributed to the dramatically different temporal profiles of inhibition these two cell types receive from amacrine cells (van Wyk et al., 2006; Russell and Werblin, 2010). However, their excitatory inputs also have some marked differences. Unlike LEDs (van

Wyk et al., 2006), which derive most of their excitatory drive from AMPA receptor currents, OFF BS RGCs (Figure 2.2) and cat β/X RGCs (Cohen, 1998) receive a significant NMDA receptor-mediated synaptic input as evidenced from their non-linear current-voltage (IV) relation.

New evidence from recordings in the guinea pig retina suggests that NMDA receptor inputs contribute to temporal contrast encoding in α and δ OFF RGCs (Manookin et al., 2010). These RGCs have large receptive fields relative to OFF BS RGCs, and represent a low spatial acuity pathway from the retina to other brain regions. However, α RGCs are distinctive for their sensitivity to motion of high spatial frequency stimuli (Demb et al., 2001b). Manookin et al., (2010) found that NMDA receptor contribution to contrast encoding varied by cell type, with α cells showing more NMDA receptor contribution to encoding lower contrast stimuli than δ cells. Similarly to α RGCs, we found that NMDA inputs in OFF BS RGCs are required for sensitivity to low contrast stimuli. By fitting OFF BS RGC IVs with a function for Mg^{2+} affinity of their NMDA receptors, we were able to estimate the magnitude of the excitatory light-evoked conductance mediated by NMDA receptors. We found that NMDA receptor inputs saturate at high contrasts, and blocking NMDA receptors disproportionately affects OFF BS RGC responses to low contrast stimuli near the threshold for detection. By pharmacologically modulating the light-evoked AMPA and NMDA receptor inputs to OFF BS RGCs, we demonstrate that saturation of the NMDA input at high contrasts is not likely to be a feature of receptor desensitization, but rather a result of selective presynaptic inhibition of the NMDA input. NMDA and AMPA receptor inputs appear to

be separated at synapses with distinct presynaptic bipolar cell terminals as evidenced from differences in their sensitivity to blocking inhibition.

To summarize, NMDA receptors make a significant contribution to contrast sensitivity in a specific type of small RGC that is thought to mediate high-acuity vision at high temporal frequencies. The NMDA input in these neurons represents a distinct excitatory pathway originating in specific bipolar cell terminals, and is useful for detecting small temporal changes in light intensity.

Materials and Methods

Tissue preparation

All procedures involving animals were done in accordance with National Institute of Health guidelines and with approval from the Oregon Health & Science University Institutional Animal Care and Use Committee. Pigmented rabbits aged 5 weeks and older were placed under dim-red illumination and sedated by intramuscular injection of ketamine (50 mg/kg) and xylazine (10 mg/kg), followed by surgical anesthesia using intravenous sodium pentobarbital (100 mg/kg). After the eyes were removed, the animal was euthanized by sodium pentobarbital injection. The anterior eye was cut away, and the portion containing the inferior retina was dissected from the rest of the eyecup. The retina, with attached pigment epithelium, was then removed. A central portion of inferior retina was gently excised, and placed photoreceptor side down in a glass-bottom recording chamber. The retina was held down with a nylon-stringed platinum-iridium wire harp. It was continuously perfused at a rate of 4-6 ml/min with bicarbonate buffered, pH 7.4, Ames medium (US Biological, Swampscott, MA) bubbled with 95% O_2/5% CO_2 heated to 36-37° C.

Ganglion cell recording and morphology

For initial identification, extracellular spike recordings were made using borosilicate glass microelectrodes of 4-6 MΩ resistance. The electrodes were filled with Ames medium and positive pressure was applied in order to clear glial processes away from ganglion cell bodies. Retinal ganglion cells were visualized through a 40x 0.75NA water immersion objective, using a video camera mounted on an upright Olympus BX-51 microscope with infrared (900 nm) differential interference contrast (IR-DIC) optics. Ganglion cell bodies within ~2mm of the visual streak were selected based on their small size, ≤15 μm diameter, and were determined to be OFF BS cells based on their spike-response characteristics (see Results). Suction was used to achieve a loose seal and improve the signal-to-noise ratio for extracellular recordings. For voltage-clamp recordings, a new electrode was filled with an intracellular solution containing (mM): 125 Cs-methylsulfonate, 6 KCl, 10 Na-HEPES, 1 EGTA, 2 Mg-ATP, 1 Na-GTP, 2.5 Na2 phosphocreatine, and 3 lidocaine N-ethyl-Cl in order to block spikes generated by voltage-gated Na channels. An empirically determined liquid junction potential of 13 mV was corrected for after the recording.

Bath-applied drugs included L-(+)-2-Amino-4-phosphonobutyric acid (L-AP4), D-(-)-2-Amino-5-phosphonopentanoic acid (D-AP5), 2,3-Dioxo-6-nitro-1,2,3,4-tetrahydrobenzo[f]quinoxaline -7-sulfonamide disodium salt (NBQX), 6-Imino-3-(4-methoxyphenyl)-1(6H)-pyridazinebutanoic acid hydrobromide (SR-95531) (Ascent Scientific, Weston-Super-Mare, UK) as well as strychnine and (1,2,5,6-Tetrahydropyridin-4-yl)methylphosphinic acid (TPMPA) (Sigma).

In experiments where N-methyl-D-aspartate (NMDA) (Tocris, Ellisville, MO) was puffed onto the ganglion cell, a glass pipette (4-6 MΩ tip resistance) was filled with 2 mM NMDA dissolved in Ames medium and positioned above an opening in the inner limiting membrane that had been created approximately 30 μm from the cell body. The puffs, 100 ms in duration, were generated using a Picospritzer microinjector (Parker Hannifin, Cleveland, OH).

In some experiments 0.4% Alexa-488 hydrazide or Alexa-488 biocytin (Invitrogen, Carlsbad, CA) were included in the intracellular solution for confirmation of cell morphology in the live tissue using a microscope-mounted CCD camera (Roper Scientfic, Tucson, AZ) or confocal microscopy in fixed tissue. Retinas in which ganglion cells were injected with Alexa-488 biocytin were fixed with 4% paraformaldehyde in 0.1 M phosphate buffer (PB) for 45 minutes, incubated successively in 10, 20 and 30% sucrose in PB and flash-frozen to -20° C on a cryostat in order to improve penetration of the tissue by the biotin conjugate. Biocytin was detected following a 48 hour (4° C) incubation with Streptavidin Alexa-488 (Invitrogen) in phosphate buffered saline containing 5% normal goat serum, 1% bovine serum albumin and 0.5% Triton X-100.

Light Stimulation

Light stimuli were generated on a computer monitor with a 60 Hz refresh rate using custom procedures implemented in Igor Pro (Wavemetrics, Lake Oswego, OR). The screen intensity was linearized in the software using a look-up table. During light stimulation, the 40x objective was replaced by a 10x, 0.25NA water immersion objective,

and the stimulus image was focused onto the photoreceptor layer. Overall stimulus intensity could be attenuated by placing calibrated neutral density filters in the light path.

The area to be used for recording was adapted for 30 minutes to the background luminance level through the 10x objective. The illuminated area was 2 mm in diameter. Light stimuli comprised a circular spot on a steady background of approximately 3×10^3 photons $\cdot s^{-1} \cdot \mu m^{-2}$ at the retina. For most experiments, the spot intensity was modulated with a square-wave time-course at one cycle per second. The background light intensity was an order of magnitude greater than steady-state rod photoreceptor saturation in the rabbit, and therefore stimuli were in the photopic range (Dacheux and Raviola, 1986; Nakatani et al., 1991). The flickering stimulus spot was varied in diameter and contrast as detailed in the *Results* section. Its contrast was defined as $C = 100 \cdot [(L_{max} - L_{min})/(L_{max} + L_{min})]$, where L_{max} and L_{min} are the maximum and minimum intensities of the spot in a stimulus sequence.

Conductance Analysis

Stimulus-activated synaptic conductance was measured from current-voltage (IV) relations obtained over a range of holding potentials between -98 and +27mV. The net light-activated synaptic IV relation was obtained by subtracting the “leak” IV relation (mean currents during the 200 ms prior to stimulus onset) from the IV relations during the light response. At positive potentials, the intracellular Cs appeared insufficient to completely suppress outward rectification, and during the voltage steps the outward currents often displayed a slow inactivation reminiscent of potassium currents (Figure 2.2

B1). This sloping baseline was subtracted from the records at positive potentials to obviate errors in measuring the amplitudes of the net light-activated synaptic currents. Synaptic inputs were resolved into two components, excitation, with a reversal potential V_E = 0mV, and inhibition, with a reversal potential at the chloride equilibrium potential, E_{Cl}, which was calculated as -68 mV under our conditions. In addition to these two linear, voltage-independent conductances, part of the excitatory input to OFF-BS-GCs was mediated by NMDA receptors, which have a non-linear IV relation due to voltage-dependent channel block by extracellular Mg ions (Mayer et al., 1984; Nowak et al., 1984). Thus, the excitatory conductance comprised linear (AMPA/Kainate) and non-linear (NMDA) components. The shape of the NMDA IV relation was measured from responses to NMDA applied to the dendrites using pneumatic pulses through a microelectrode containing 2 mM NMDA (Figure 2.2 B). Therefore, three conductances were required to account for the measured IV relations. The magnitude of the conductances were obtained by performing a least-squares fit to synaptic IV relations using the equation:

$$I(V) = G_i(V - E_{Cl}) + \left(G_e + G_{NMDA} f(V)\right)(V - V_E), \qquad \ldots 1$$

where, V is the membrane potential, G_i is the inhibitory conductance, E_{Cl} is the chloride reversal potential, G_e is the linear excitatory component, or non-NMDA component, V_E is the excitatory reversal potential, G_{NMDA} is the non-linear NMDA component and $f(V)$ is the fraction of conducting NMDA channels as a function of voltage. The function, $f(V)$, which accounts entirely for any non-linearity of the synaptic IV relations, was evaluated as;

$$f(V) = 1 - \frac{[Mg]}{\left([Mg] + K_{Mg} e^{(V/V_\delta)}\right)} \qquad \ldots 2$$

where, the extracellular magnesium concentration, [Mg]= 1.2 mM, K_{Mg} is the apparent Mg binding affinity at zero millivolts, and V_d, is proportional to the fraction of the membrane electric field sensed by the Mg ion at the binding site. K_{Mg} and V_d were evaluated from fits to the measured NMDA IV relations (K_{Mg} = 14 mM and V_d = 21 mV, Fig. 2B), and these values were held constant when evaluating the NMDA component in the synaptic IV relations. The value for V_d is equivalent to Mg binding 63% across the membrane electric field, which compared well with some previously published estimates for NMDA channels (Mayer and Westbrook, 1985; Chen and Huang, 1992). However, K_{Mg} was somewhat larger than previous estimates, indicating an unusually low magnesium binding affinity (See Results and Discussion).

Statistical Analysis

Conductance analysis was performed on current traces from individual cells, and mean conductance plots are shown with 95% confidence intervals (1.96 * standard error of the mean, SEM) for each time-point sample in the IV relations. Plots of IV relations and conductance integrals show SEM. Paired Students' t-tests were used to assess the statistical significance of drug application on the magnitude of conductances. Repeated measures analyses of variance (RM ANOVA) were used for comparisons across more than two groups, such as the effect of multiple stimulus intensities. In all significance tests, the statistical levels for rejecting the null hypothesis were $p < 0.05$.

Results

Identifying OFF brisk-sustained RGCs

We targeted OFF BS RGCs in the whole-mount retina by selecting cells with somas less than 15 μm diameter. In IR-DIC view, BS cells have a semi-circular nucleus and overall the soma appears very similar to that of LEDs (van Wyk et al., 2006). However, OFF BS RGCs have a less prominent nucleus than either LEDs, or the ON BS RGCs. The cell type of a targeted cell was confirmed by recording extracellular action potentials (spikes) elicited by a centered, square-wave flickered light spot (Figure 2.1 A). A saturating-strength, circular stimulus (greater than 40% contrast) restricted to the receptive field center evoked a peak firing rate of over 200 spikes per second within the first few spikes. The latency to the peak firing rate was approximately 85 ms. As with many rabbit RGC types in the whole-mount preparation, BS RGCs did not fire action potentials in the presence of steady, bright background illumination (Amthor et al., 1989b).

The concentric, center-surround organization of the receptive field was confirmed by flashing centered spots of increasing diameter. Cells were recorded approximately 1 mm ventral to the visual streak, and the diameter of the receptive field center, as determined by fitting a difference of Gaussians function to the stimulus diameter-response plots, averaged 130 ± 12 μm (mean ± standard deviation; n = 141, Figure 2.1B). In the same group of cells, the diameter of the surround inhibition based on the negative Gaussian space constant averaged 460 ± 36 μm. These values compare favorably with previous estimates (Vaney et al., 1981a; Devries and Baylor, 1997). In line with previous work (Amthor et al., 1989b; Roska and Werblin, 2001; Roska et al., 2006) our physiologically

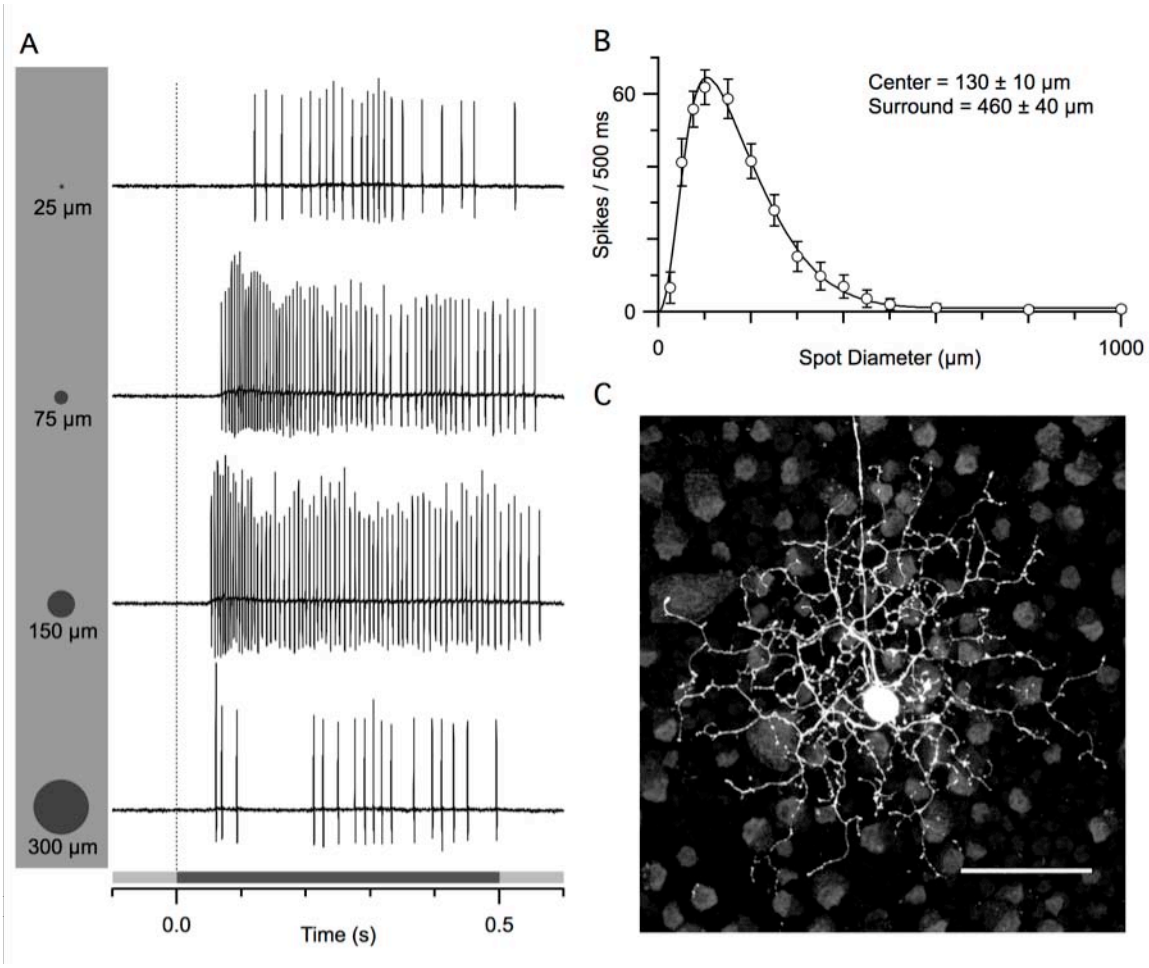

Figure 2.1. Physiological and anatomical properties of OFF BS RGCs.
A, Spiking of an individual OFF BS RGC in response to a dark spot flashed for 0.5 s. During the largest responses, for 75 and 150 µm diameter spots, the cell reached a peak firing rate within 100 ms of stimulus onset, and maintained firing for the duration of stimulus presentation.
B, Mean spike output versus stimulus diameter for 141 OFF BS RGCs. The smooth line shows the fit to a difference of Gaussians. The diameter of the receptive field center was estimated as 2σ of the positive Gaussian. The diameter of the inhibitory surround is 2σ of the negative Gaussian.
C, Confocal micrograph of the neuron in A. Scale bar = 50 µm.

identified OFF BS RGCs displayed a consistent and distinct anatomical structure, as revealed by epifluorescent view following recording (n = 14) and a confocal photomicrograph of a fixed fluorophore-filled cell (Figure 2.1 C). The dendrites branched profusely and irregularly, stratifying broadly in the OFF sub-lamina of the inner

plexiform layer (IPL), and matched in extent the physiological receptive field. Anatomically, OFF BS RGCs most likely correspond to cell type G4 described by Rockhill and colleagues (2002), or cell type III.3 described by Famiglietti (2005).

RGCs similar to OFF BS RGCs have been identified anatomically as β-cells, and physiologically as X-cells in cat retina (Enroth-Cugell and Robson, 1966; Cleland et al., 1971; Boycott and Wassle, 1974; Hochstein and Shapley, 1976b). Excitation of cat and ferret X-cells is driven in part by NMDA receptors, which display a highly non-linear current-voltage relation due to voltage-dependent magnesium block (Cohen et al., 1994; Cohen, 1998; 2000). Other RGC types, such as ON α-like ganglion cells in the mouse and guinea pig (Pang et al., 2003; Manookin et al., 2010), as well as the LEDs in the rabbit may lack significant NMDA receptor-mediated contributions in their light-evoked excitation (van Wyk et al., 2006; 2009). Even so, the significance of NMDA receptors to visual information processing in specific RGCs has not been extensively studied. The goal of this study was to define the role of NMDA receptors in generating receptive field properties of OFF BS cells.

NMDA receptor mediated inputs to OFF BS cells

The excitatory centers of OFF BS RGCs were stimulated with a square-wave contrast-reversing spot at 1 Hz. To obviate stimulation of the surround, the diameter of the spot, 100 to 150 μm, was set smaller than the extent of the dendritic field. We recorded light-evoked whole-cell currents at a series of voltages, and the resultant current-voltage (IV) relation showed strong outward rectification, consistent with an NMDA receptor contribution, as has been reported in cat β-cells (Cohen, 2000) (Figure

2A). In order to quantify the contribution of NMDA receptors to the total light responses, we had to delineate the non-linear (NMDA receptor-mediated) component from the linear excitatory (AMPA/KAinate) and inhibitory components (See Materials and Methods). The shape of the non-linear NMDA current-voltage relation was determined by measuring the peak current elicited by focal 2 mM NMDA puffs in the presence of 100 μM CdCl to block synaptic transmission and prevent glutamate release from bipolar cell terminals (Figure 2.2 B). The suppression of the inward current at hyperpolarized potentials due to voltage-dependent extracellular Mg^{2+} block can be accounted for by a sigmoidal binding function with two coefficients, one specifying the apparent Mg^{2+} binding affinity at 0 mV (K_d), and the other accounting for the equivalent fraction of the membrane electric field sensed at the binding site (V_d, See Materials and Methods for equation). The values of these coefficients for NMDA receptors in OFF BS RGCs were obtained from fits to the NMDA puff IV relations (Figure 2B). The apparent K_d was between 7 and 28 mM with a mean of 14 mM, which means that on average half of the NMDA receptors are blocked at ~ -51 mV, and the V_d was 21 ± 2 mV, which is equivalent to a binding site 63 ± 6% across the membrane electric field. While the V_d is similar to previous estimates (Mayer and Westbrook, 1985; Chen and Huang, 1992), the apparent K_d is approximately two fold higher than was first reported in cultured cortical neurons (Ascher and Nowak, 1988; Johnson and Ascher, 1990). However subsequent studies showed that the K_d of some NMDA receptors in the brain may be much higher due to differences in subunit composition (Monyer et al., 1994), and the K_d reported for other RGC types of 18 mM is similar to what we found (Manookin et al., 2010). If the non-linearity observed in the net light-activated IV relation is due entirely to NMDA

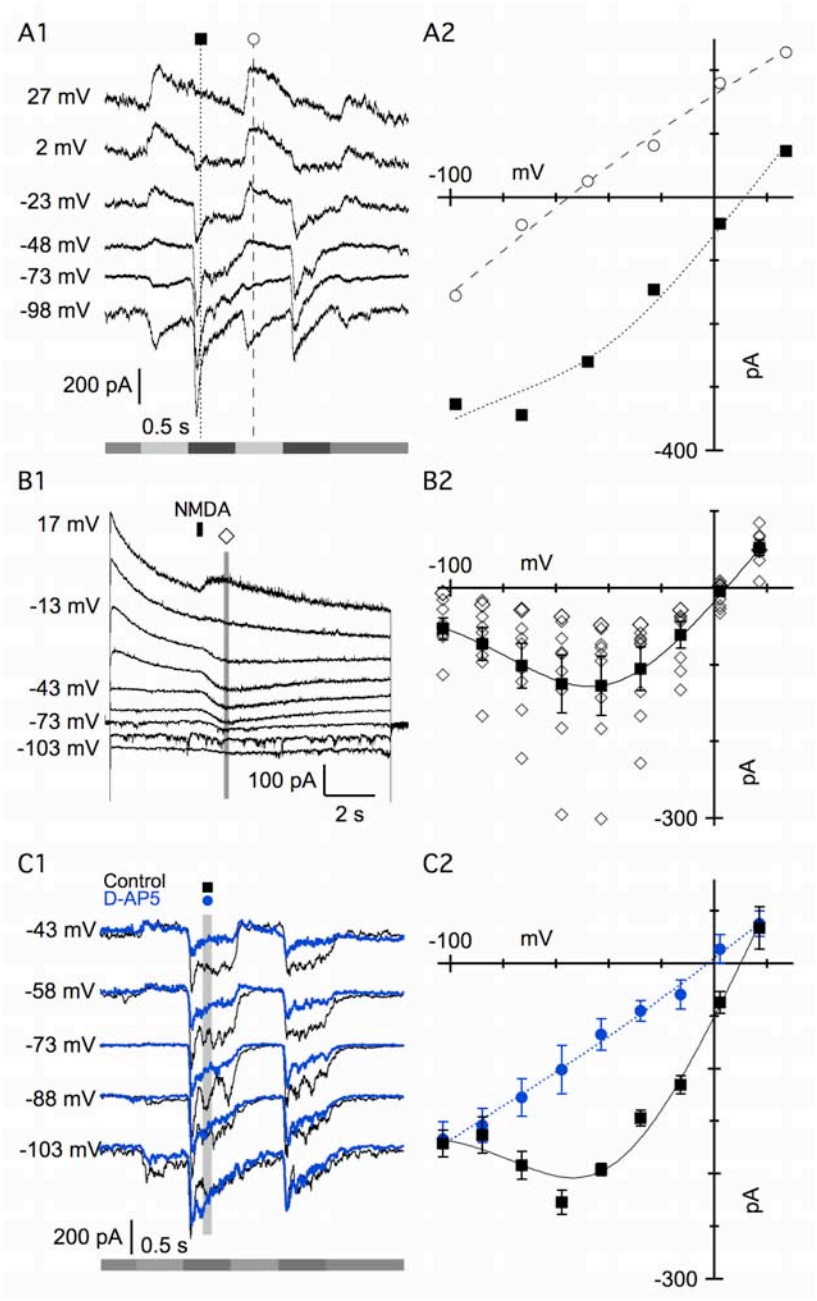

Figure 2.2 NMDA receptors contribute to excitation in OFF BS RGCs.

A1, Current traces recorded from a single OFF BS RGC voltage-clamped at the indicated membrane potentials. The shading of the bars underneath the traces represents the temporal progression and intensity of the stimulus in this and subsequent figures.

A2, Leak-subtracted currents from A1 are plotted against holding potential. Currents were measured at the onset of the dark phase of the stimulus (square) and the bright phase (circle). Note non-linearity in IVs.

B1, Voltage-clamped responses of a single OFF BS RGC to puffs of 2 mM NMDA. Black bar indicates timing of puff. Gray bar indicates period where the IV in B2 was measured.

B2, Individual IVs of the puff responses of 6 OFF BS RGCs. The dark squares represent the average currents at each voltage ± SEM.

C1, Representative current traces in the presence of bath-applied 50 µM D-AP5 (blue) and matched controls (black).

C2, Mean IVs for D-AP5 and control conditions (n=8). NMDA receptor block linearized the IV.

receptor activity, then blocking NMDA receptors should produce a linear IV relation. This expectation was confirmed by applying a saturating concentration of the NMDA receptor antagonist *D*-AP5 (50 μM). The residual IV relation during the negative contrast phase (blue circles, Figure 2.2 C2) was linear and reversed very close to 0 mV, consistent with a linear excitatory AMPA/KAinate input, and no detectable inhibitory input. The IV relations were resolved into excitatory and inhibitory components over the full duration of the light stimuli in a larger group of 32 cells (Figure 2.3 A). During the positive contrast phase of the stimulus, the synaptic currents appeared to reverse close to E_{Cl} in individual cells (Figure 2.2 A2), and on average, the synaptic input was dominated by inhibition (Figure 2.3 A, red trace). During the negative contrast phase, synaptic input was dominated by excitatory conductances (Figure 2.3A, black trace), however, the currents reversed positive to 0 mV (Figures 2.2 A2 and C2, black squares), which was accounted for by a decrease in a tonic inhibitory input present under steady background illumination, i.e. a linear conductance with a negative slope having a reversal potential at E_{Cl}. The data shown in chapter 3 provide further support for this interpretation and indicate that the tonic inhibition is glycinergic.

The NMDA receptor-mediated conductance boosts sensitivity at low contrasts and shows less contrast adaptation than the AMPA/KA excitatory conductance

The excitatory component (Figure 2.3 A), is resolved into the linear AMPA/KA and non-linear NMDA components in Figure 3B. The integral of the NMDA component during the OFF-phase of the first stimulus cycle was 1.7 ± 0.12 nS (n = 32), 1.9 ± 0.16 nS and 1.7 ± 0.24 nS at 10%, 20% and 60% contrast respectively, whereas the integral of the

AMPA/KA excitatory conductance increased from 0.6 ± 0.04 nS at 10% contrast to 1.0 ± 0.07 nS and 2.4 ± 0.1 nS for the two stronger stimuli. Thus, the NMDA receptor mediated excitation appeared to saturate at contrasts below ~ 20%, while the AMPA/KA component showed a steady increase over the same contrast range (Figure 2.3 C). A possible explanation for the rapid contrast-dependent saturation of the NMDA component is the high glutamate affinity relative to AMPA/KA receptors. However, in 6 out of the 32 OFF BS RGCs tested, the NMDA receptor component increased with stimulus strength, similarly to the AMPA/KA component (Data not shown), which suggests that NMDA receptor binding is not necessarily saturated at low contrasts.

Comparison of the integrals of the first and second stimulus cycles reveals that contrast adaptation is weaker for the NMDA input than the AMPA/KA inputs (Figure 2.3 D). At each of the three stimulus intensities tested in increasing order, the integral of the AMPA/KA component during the second stimulus cycle decreased to 0.62 ± 0.03, 0.67 ± 0.03, and 0.62 ± 0.04 of the first cycle ($p < 0.05$; null hypothesis = 1.0), while the NMDA component, by the same measure, did not show significant adaptation (ratios: 0.90 ± 0.04, 0.94 ± 0.04 and 1.13 ± 0.19).

If NMDA receptors constitute a larger portion of the excitatory conductance at low contrasts, then this property should be mirrored by their contribution to the RGC spike output. Blocking NMDA receptors with 50 μM *D*-AP5 completely suppressed the NMDA conductance, but had little or no effect on the AMPA/KA conductances (Figure 2.4 A), which allowed us to use *D*-AP5 to assess the contribution of NMDA receptors to the spiking properties. *D*-AP5 suppressed the number of spikes

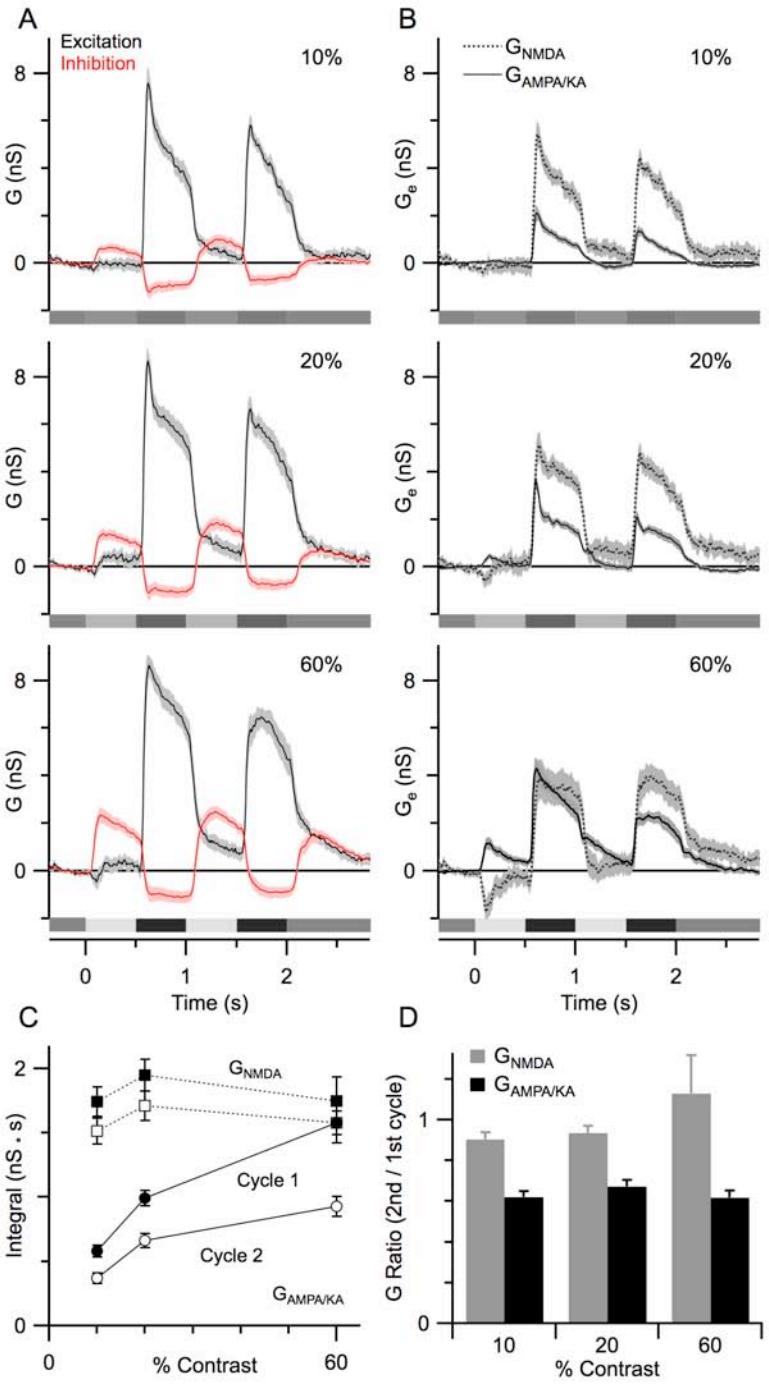

Figure 2.3. AMPA/KA and NMDA components of excitation differ in their contrast sensitivity and adaptation.
A, Plots of mean total excitatory and inhibitory conductance components of 32 OFF BS RGCs evoked by a focal stimulus flickered at 2Hz with stimulus contrasts of 10% (top), 20% (middle) and 60% (bottom).
B, Plots of NMDA and AMPA/KA components of the excitatory conductance from the experiment in A.
C, Integrals of conductances from B plotted against contrast. Filled symbols represent integrals of first response cycle; open symbols – second cycle. AMPA/KA component (bottom) increased with contrast, while NMDA component did not (top).
D, Measure of contrast adaptation from first to second stimulus cycle. The integral of the conductance in response to the second stimulus cycle is normalized to the response to the first. AMPA/KA input showed adaptation from first to second cycle, while NMDA component did not.

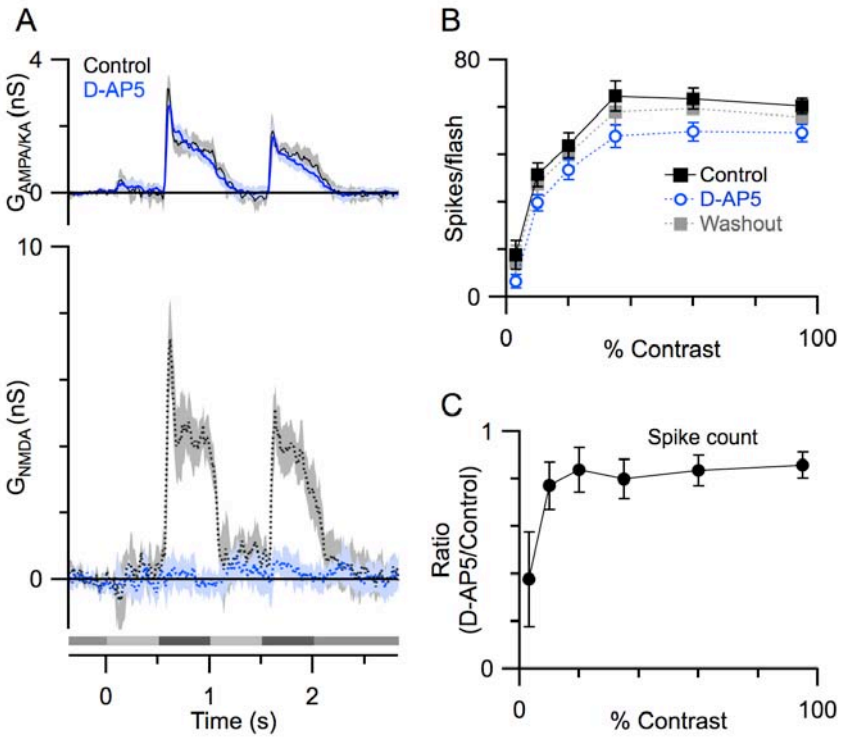

Figure 2.4. NMDA receptors contribute to low contrast detection in OFF BS RGCs. **A,** Mean traces of AMPA/KA (top), and NMDA (bottom) components of excitatory conductance in 8 OFF BS RGCs under control conditions (black) and with bath applied 50 µM D-AP5 (blue) evoked by a 20% contrast stimulus. D-AP5 blocked the NMDA component. **B,** Means of spike output from 5 OFF BS RGCs plotted against stimulus contrast. Black symbols represent control conditions, blue − D-AP5 in the bath, and gray are drug washout. **C,** Plot of mean spike output in the presence of D-AP5 from B normalized to control. D-AP5 suppressed spiking most strongly at the lowest contrast.

activated during the first stimulus cycle of a 1Hz stimulus at all contrasts, an effect that was readily reversible (Fig. 2.4 B). During the first and second stimulus cycles, *D*-AP5 suppressed spiking by 62% (SEM = 20%; n=5) of control at 3% contrast, but only decreased the spike count by 20-25% of control at higher contrasts (Figure 2.4 C). Although the NMDA conductance represented between ~75% and 40% of the total excitatory conductance (10% and 60% contrast), due to the Mg block, NMDA receptors

are predicted to contribute only ~ 35% to 20% of the synaptic current near the resting potential (~ -60mV). The actual contribution could be larger, as depolarization during synaptic responses relieves the voltage-dependent Mg-block, however, the predicted NMDA currents are in rough agreement with the ~ 20% block of spiking. In summary, NMDA inputs appear to be particularly important for generating responses to stimuli that are close to the threshold contrast measured for rabbit and guinea pig RGCs in other studies (Merwine et al., 1995; Xu et al., 2005b), but saturate rapidly and drive less of the spiking at intermediate and high contrasts.

NMDA and AMPA/KA excitatory conductance components are differentially regulated by presynaptic inhibition

Conductance analysis revealed the presence of significant inhibitory input to the center receptive field of OFF-BS RGCs, and we used specific antagonists in order to determine the receptors involved. These experiments provided evidence for marked presynaptic inhibitory modulation of the excitatory inputs. In the presence of the glycine receptor antagonist, strychnine (1 μM), the AMPA/KA conductance component was significantly suppressed ($n = 6$, $p < 0.05$) at all stimulus contrasts, however, the NMDA component was significantly suppressed only at 20% contrast ($p < 0.05$ Figure 2.5 A and B). This suggests that the magnitude of the AMPA/KA component is modulated by glycinergic pathways. The lack of suppression of the NMDA component indicates that the effects cannot be due simply to block of the rod-pathway between the AII amacrine cell and the Off-cone-bipolar cells. Applying $GABA_A$ and $GABA_C$ receptor blockers had

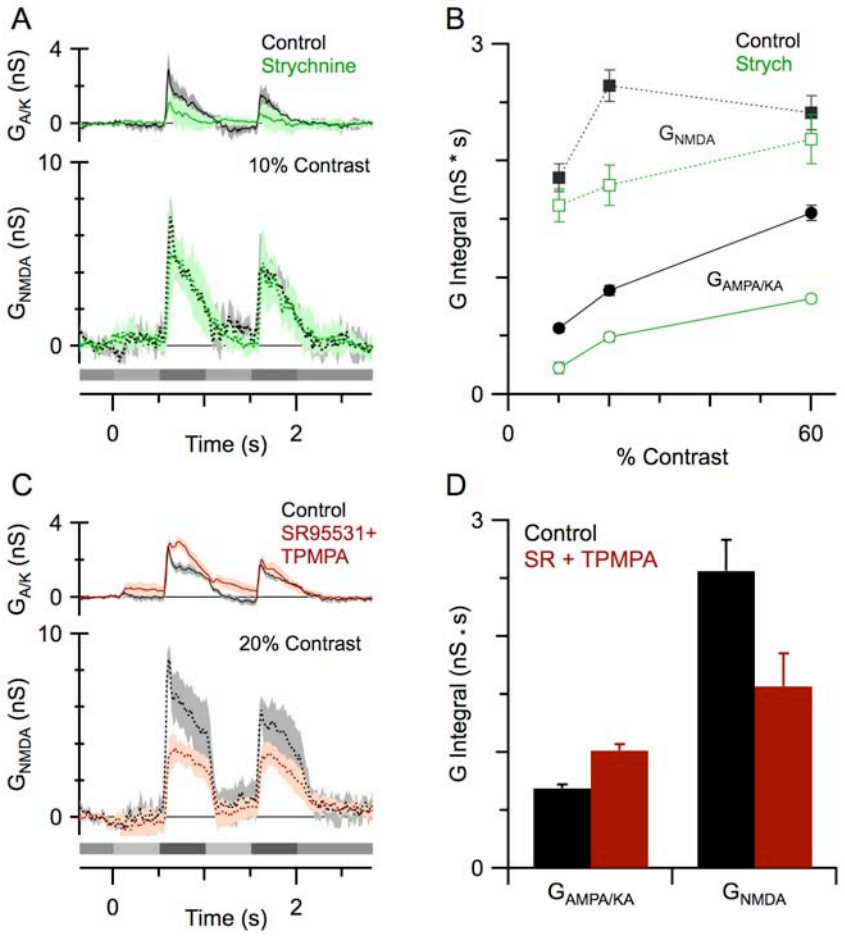

Figure 2.5. NMDA and AMPA/KA excitatory inputs are modulated differently by presynaptic inhibition.

A, Mean AMPA/KA (top), and NMDA (bottom) components of excitatory conductance derived from voltage-clamp recordings of 6 OFF BS RGCs under control conditions (black) and with bath applied 1 µM strychnine (green) evoked by a focal stimulus at 10% contrast.

B, Means of the integrals of excitatory conductance evoked by the first stimulus cycle plotted against stimulus contrast. Strychnine consistently attenuated the AMPA/KA component, while NMDA was only reduced at 20% contrast

C, Same as A, with 25 µM SR95531 and 50 µM TPMPA in the bath (stimulus contrast was 20%; n=10).

D, Mean integrals of the AMPA/KA and NMDA components evoked by the first stimulus cycle in C. $GABA_A$ and $GABA_C$ antagonists significantly attenuated the NMDA component while increasing the AMPA/KA component ($p < 0.05$).

opposite effects; the AMPA/KA component was significantly increased at 20% contrast while the NMDA component was suppressed ($n = 10$, $p < 0.05$, Figure 2.5 C and D). Together this evidence suggests that the bipolar cell terminals driving the AMPA/KA component are preferentially inhibited via GABAergic mechanisms, while NMDA inputs are more likely to be modulated presynaptically via glycinergic mechanisms. As noted above, blocking NMDA receptors did not affect the amplitude or time-course of the AMPA/KA conductance, showing that NMDA receptors do not play a role in presynaptic inhibition, at least at the spatial scale of these experiments. We then tested whether inhibitory inputs modulating the NMDA component are mediated via AMPA/KA transmission.

Application of the AMPA/KA antagonist NBQX (25 μM), completely suppressed the linear portion of the excitatory conductance (Figure 2.6 A − C), and produced an increase in the magnitude of the NDMA component at moderate to high (60%) contrast ($p < 0.05$; $n = 6$, Figure 2.6 B − D). These results were unexpected, since synaptic transmission from cones to OFF bipolar cells involves AMPA or kainate receptors and therefore should be blocked by NBQX (Saito and Kaneko, 1983; DeVries, 2000). In contrast we found that synaptic transmission was maintained in the presence of CNQX or NBQX even at concentrations as high as 100 μM (data not shown). The NBQX-resistant excitatory input to OFF RGCs did not originate from the ON pathway, because the NMDA component was maintained in the presence of L-AP4 (see Figure 3.1 A1 below). We therefore concluded that it originated from OFF cone bipolar cells that were not inhibited by NBQX within the time frame of the recording.

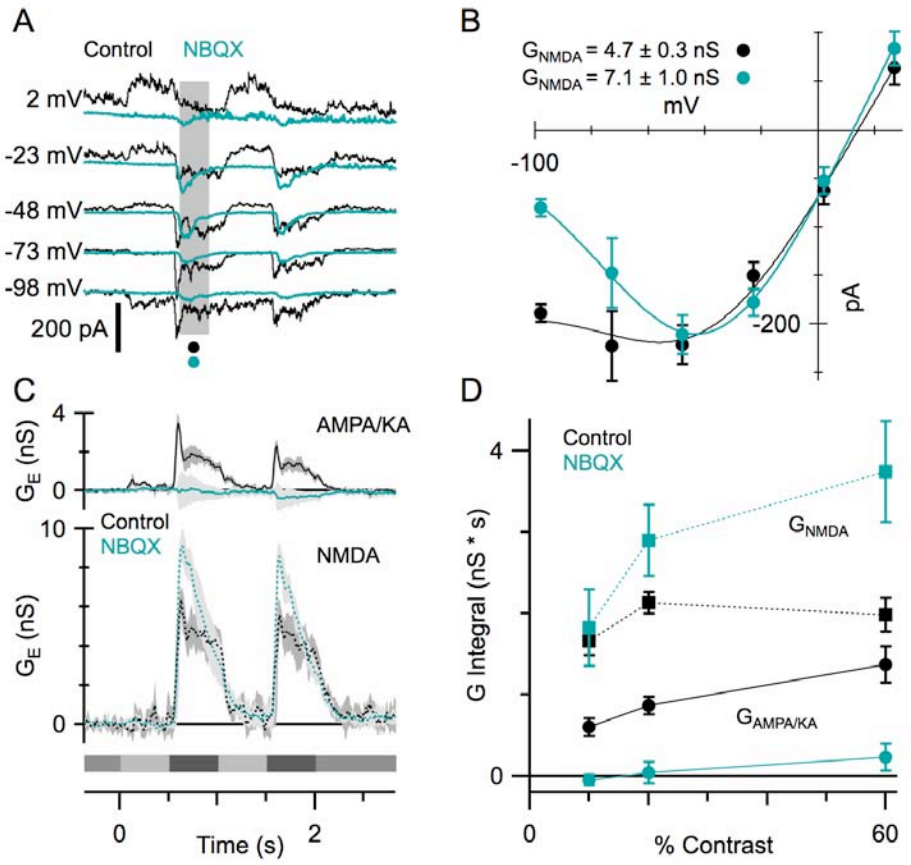

Figure 2.6. Blocking AMPA/KA receptors increased the NMDA receptor input at high stimulus contrasts.

A, Current (cyan traces) recorded with bath-applied 25 µM NBQX in a single OFF BS RGC voltage-clamped at the indicated membrane potentials matched with control current traces (black). Temporal contrast of the stimulus was 20% . Current in the shaded area was averaged for IV in B.

B, Mean light-evoked, leak-subtracted IV for control and NBQX conditions. The NMDA component is significantly larger with NBQX ($p<0.05$).

C, Mean AMPA/KA (top), and NMDA (bottom) components of excitatory conductance derived from voltage-clamp recordings of 6 OFF BS RGCs under control conditions (black) and with NBQX (cyan).

D, Means of the integrals of excitatory conductance evoked by the first stimulus cycle plotted against stimulus contrast. Blocking AMPA/KA receptors increased the NMDA component for high contrast stimuli ($p < 0.05$ for 60% contrast).

With complete suppression of AMPA/KA receptors, the integral of the NMDA component increased at higher contrasts and the contrast sensitivity resembled that of the AMPA/KA component under control conditions (Figure 2.6 D). This strongly suggests that the invariance of the NMDA component as a function of contrast, observed under control conditions, is not due to receptor saturation, but rather due to presynaptic inhibition by amacrine cells driven by AMPA/KA receptors.

Discussion

Two excitatory retinal pathways, one driven by AMPA receptors and the other driven by NMDA receptors combine in a single RGC to shape the temporal response features of its receptive field center. The different intensity-response relations for the NMDA and AMPA/KA excitatory input components (Figure 2.3 C) raise the possibility that these receptors are not activated by a common input. Two lines of evidence support the hypothesis that there are separate NMDA and AMPA/KA pathways. First are differences in contrast adaptation between the AMPA/KA and NMDA components of excitation, and second are differential effects of inhibitory antagonists. Thus, excitation in OFF BS RGCs consists of two inputs with distinct contrast gain and adaptation profiles. NMDA receptor inputs are strongly suppressed by presynaptic inhibition at higher stimulus contrasts, and make a significantly larger contribution to the spike output of OFF BS RGCs at low contrasts.

NMDA receptor input boosts OFF BS RGC response to low stimulus contrasts

NMDA receptors contribute to light-evoked RGC spike output in salamander, cat, and rabbit (Slaughter and Miller, 1983a; Massey and Miller, 1990; Mittman et al., 1990; Diamond and Copenhagen, 1993; Cohen et al., 1994). Different classes of RGCs show distinct patterns of NMDA receptor expression, which may contribute to the differences seen in signal encoding among retinal pathways (Manookin et al., 2010). In particular, NMDA receptors in ON and OFF RGCs vary in subunit composition, with ON RGCs expressing NMDA receptors perisynaptically and OFF RGCs showing synaptic localization (Chen and Diamond, 2002; Sagdullaev et al., 2006; Zhang and Diamond, 2009). This raises the possibility that differences in NMDA receptor expression may contribute to functional asymmetries observed between ON and OFF pathway outputs (Chander and Chichilnisky, 2001; Kim and Rieke, 2001; Chichilnisky and Kalmar, 2002; Zaghloul et al., 2003).

The present study demonstrates that NMDA receptor-mediated synaptic excitation has a very nonlinear contrast response in rabbit OFF BS RGCs. At a low stimulus contrast, 10%, the NMDA input is relatively large, and its contribution to excitation does not increase much in response to stronger stimuli. Consequently, blocking NMDA receptors suppressed significantly more spikes at the lowest contrast tested, than at moderate or saturating contrasts, suggesting that the role of NMDA receptors in OFF BS RGCs is to specifically boost responses to weak stimuli. In order for NMDA receptors to drive spiking when inputs from other glutamate receptors are weak, NMDA receptors would have to conduct current near the cell's resting potential. Indeed, we determined that NMDA receptors native to OFF BS RGCs produce agonist-evoked currents down to

-80 mV, which is likely due to two fold lower Mg^{2+} affinity than commonly found in cortical neurons (Johnson and Ascher, 1990).

NMDA and AMPA mediated inputs represent separate excitatory pathways

The magnitude of the NMDA component was essentially invariant from 10 to 60% contrast. This apparent saturation of the NMDA component was relieved when AMPA receptors were blocked by NBQX, resulting in a contrast-dependent increase in the NMDA component. We propose that the effect of NBQX was indirect, produced by blocking amacrine cell mediated inhibition of bipolar cell terminals. Yu and Miller (1996) reached a similar conclusion to explain how NBQX increased light-evoked NMDA inputs in salamander RGCs. If NBQX acts by reducing presynaptic inhibition, similar effects might be achieved by blocking of inhibition. Blocking $GABA_A$ receptors actually decreased the NMDA input, while the AMPA/KA component was potentiated. Thus, these experiments revealed that AMPA inputs are also subject to presynaptic inhibition, but in contrast to the NMDA input, GABA receptor antagonists increased the AMPA input suggesting that GABA receptors mediate inhibition of bipolar cell terminals presynaptic to AMPA receptors. The experiments were performed at sub-saturating stimulus intensities, indicating that the differences cannot be due to saturating non-linearities.

The effects of glycine receptor block were not as clear as for GABA receptors, but there also appeared to be an inverse effect. The NMDA input was unaffected by glycine receptor antagonist strychnine at the lowest and highest intensity tested, while the AMPA input was strongly suppressed by strychnine at all contrasts. It is unclear why strychnine did not enhance the NMDA input as did blocking AMPA/KA receptors with NBQX. It is

possible that antagonizing glycine receptors throughout the retina could have increased other sources of inhibition that are not ordinarily active. However, both drugs had the effect of removing the apparent saturation of the NMDA component at high stimulus intensities, suggesting that they both blocked presynaptic inhibition (See diagram in Figure 2.7).

Although our background light intensity was near photopic levels for rabbit photoreceptors, a dimming light stimulus could conceivably have affected rod bipolar cell output, which increases OFF bipolar output via the glycinergic AII amacrine cell (Dacheux and Raviola, 1986). The different effects of strychnine on the AMPA/KA and NMDA inputs indicates that the effects of strychnine cannot be attributed to suppression of signaling through the rod-pathway.

In sum, the differential and sometimes opposite effects of the inhibitory antagonists are inconsistent with the idea that the NMDA and AMPA/KA receptors are colocalized, and exposed to the same source of glutamate. This provides strong evidence for the segregation of the receptors to separate synapses.

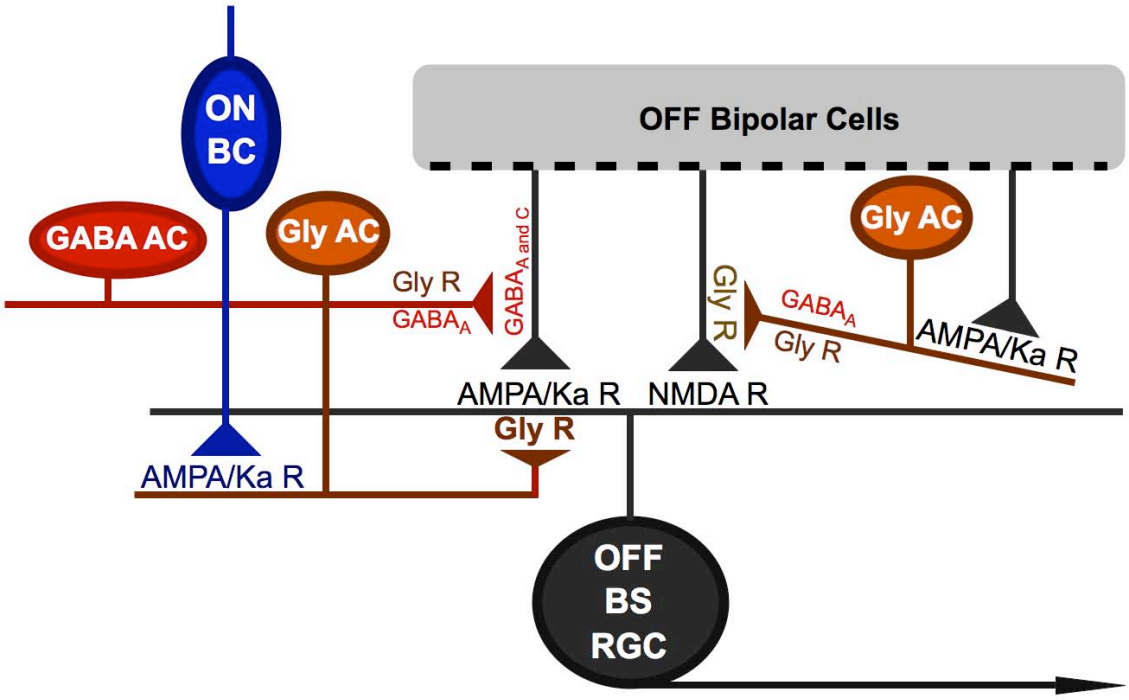

Figure 2.7 NMDA and AMPA/KA receptors may be segregated to different synapses.

The OFF bipolar cell terminal that receives GABAergic inhibition (left) is presynaptic to AMPA/KA receptors. The one on the right receives primarily glycinergic inhibition and forms synapses with a high concentration of postsynaptic NMDA receptors. The presynaptic glycinergic amacrine cell is excited by AMPA/KA receptors. Therefore if AMPA/KA receptors are blocked (Figure 2.6), the bipolar cell providing glutamate at NMDA receptor synapses is disinhibited. Likewise, blocking GABA receptors removes some inhibition from the bipolar cell terminal on the left, increasing AMPA/KA input to the OFF BS RGC, while also potentially making the glycinergic amacrine cell less inhibited, leading to a smaller NMDA component. Amacrine cells may express receptors for both glycine and GABA and receive some tonic input from other GABAergic and glycinergic cells. Therefore, if one type of receptor is blocked, the inhibition driven by other type is enhanced. Such a scheme would lead to the differential effects of inhibition seen in Figure 2.5.

The glycinergic amacrine cell on the left provides the OFF BS RGC with a feedforward inhibitory input from the ON channel. The properties of this input are discussed in Chapter 3.

Chapter 3

ON pathway inhibitory input contributes to high frequency responses and contrast adaptation in OFF BS RGCs

Ilya Buldyrev and W. Rowland Taylor

Introduction

As in other sensory systems, information flow through the visual system is segmented into parallel channels, which, in the retina, comprise the output from multiple classes of ganglion cells. Each class of ganglion cell represents a distinct spatio-temporal filter that extracts specific information from the visual scene. Parallel channels arise at the first visual synapse, with multiple classes of bipolar cells that relay information from photoreceptors to retinal ganglion cells (RGCs) (Reviewed by Wassle, 2004). A further level of complexity is added by connections from amacrine cells in the inner plexiform layer (IPL) of the retina, which display a much larger diversity of type and function than either the bipolar cells or RGCs (Young and Vaney, 1990; MacNeil et al., 1999). The goal of the study presented in this chapter was to determine how inhibitory synaptic inputs to the receptive field center determine the temporal response properties of OFF brisk-sustained (BS) RGCs in the rabbit retina.

We found a novel crossover connection from ON bipolar cells to OFF BS RGCs via a yet to be identified glycinergic amacrine cell type, which is driven by ionotropic glutamate receptors. Unlike the dis-inhibition produced by the ON input in OFF α RGCs, which appears to account for some of the sensitivity of these OFF cells to low contrast

stimuli (Manookin et al., 2008), the ON-driven input to OFF BS RGCs increases their sensitivity to high temporal frequencies.

Materials and Methods

The tissue preparation, ganglion cell recording, and statistical analysis were the same as described in the *Materials and methods* section of Chapter 2.

Light Stimulation

The general setup for delivering light stimuli was the same as described in Chapter 2. The notable difference is that both the temporal contrast and temporal frequency of the stimulus were varied. The frequency values in Hz shown in Figure 3.2 represent the frequency at which the spot transitioned from bright to dark and the reverse. The frequency of the entire stimulus cycle was half of this value.

Analysis

We found that spontaneous inhibitory synaptic inputs dominated the membrane current variance in OFF-BS cells under background illumination. This afforded the opportunity to check the linearity and reversal potential of the inhibitory inputs by measuring the IV relation of these membrane current fluctuations. The magnitude of the current fluctuations, calculated from high-pass filtered current traces (F_{pass} = 10Hz), were minimal at -69 mV, which is close to E_{Cl}, and increased linearly with voltage above and below E_{Cl} (Figure 3.1 D and E). Applying the glycine and $GABA_A$ receptor antagonists strychnine and SR95531 reduced the noise at all membrane voltages to the baseline value

observed at E_{Cl} (Figure 3.1 D). Thus, there was minimal contribution to the membrane current noise from glutamatergic inputs. Blocking AMPA glutamate receptors with NBQX did not affect the amplitude of the noise at E_{Cl}, suggesting that there was little or no tonic excitatory input present (Figure 3.1 E).

Results

ON pathway glycinergic inhibition provides light-evoked and tonic inhibitory input

OFF RGC have been shown to receive inhibition from the ON pathway, both as a direct input, and presynaptically (Wassle et al., 1986; Molnar and Werblin, 2007; Manookin et al., 2008; Liang and Freed, 2010). It has been proposed that such inhibition, termed crossover inhibition, is mediated by AII amacrine cells, and serves to increase gain and enhance rectification of OFF RGC responses (Manookin et al., 2008; Molnar et al., 2009; van Wyk et al., 2009). Here, we observed that the majority of stimulus-evoked inhibition in OFF BS RGCs originates from ON bipolar cells (Figure 3.1), since application of 100 μM L-AP4, which blocks the ON pathway by maximally activating mGluR6 receptors (Slaughter and Miller, 1981; Nawy and Jahr, 1990), blocked the inhibitory conductance during the bright phase of the stimulus (Figure 3.1). L-AP4 had very little effect on the excitatory inputs (Figure 3.1 A1, lower graph), indicating that the ON-pathway does not mediate inhibition of the bipolar cells presynaptic to the OFF BS RGCs. In part because crossover inhibition is insensitive to AMPA/KA antagonists (Manookin et al., 2008), previous studies concluded that the AII amacrine cell was the only possible source, since these amacrine cells are unique in making excitatory gap junction connections with ON bipolar cell terminals (Kolb and Famiglietti, 1974; Deans et al., 2002; Veruki and Hartveit, 2002). However, crossover inhibition in OFF BS RGCs

was abolished by blocking AMPA/KA receptors with NBQX (Figure 3.1 A2), suggesting that the glycinergic amacrine cells providing ON pathway inhibition are driven by conventional glutamatergic inputs from ON bipolar cells. Strychnine blocked all inhibition, suggesting that crossover inhibition, and OFF pathway mediated inhibition are glycinergic (n=4, Figure 3.1 B1). The addition of SR95531, the $GABA_A$ receptor antagonist, produced very little additional change, confirming that the light-evoked inhibitory inputs to the RGCs as determined using our conductance analysis method consist almost entirely of glycinergic inputs (Figure 3.1 B2).

The 1 nS of negative inhibitory conductance elicited during the dark phase of the stimulus requires the presence of at least 1nS of tonic inhibition, and since strychnine blocks light-evoked inhibition (Figure 3.1 B1), we expected it would also block ~ 1nS of tonic conductance. However, strychnine blocked only 0.27 ± 0.04 nS ($p < 0.05$), while co-application of strychnine with the $GABA_A$ receptor antagonist SR95531 blocked 1.05 ± 0.12 nS ($n = 4$, $p < 0.05$) of tonic inhibitory conductance (Figure 3.1 C). The inability of strychnine to block the expected 1 nS could be explained if it caused an increase in a GABAergic input that is not normally present. SR95531 alone had no significant effect on the light-evoked inhibitory inputs generated by center stimulation (Data not shown).

Tonic inhibition is also evident from measurements of the current variance under background illumination at a range of membrane potentials. The magnitude of the current variance varied linearly with voltage, reaching a minimum at E_{Cl}, suggesting that the current noise is dominated by background inhibitory input (See Methods for details). Strychnine reduced the current noise to 91 ± 13% of control ($n = 7$, $p > 0.05$), while a combination of strychnine and SR95531 decreased the current noise to 7 ± 4% of control

levels (n = 8, $p < 0.05$, Figure 3.1 D). The apparent discrepancy between the amount of the tonic conductance (~ 25%) and the variance (less than 10%) blocked by strychnine could be explained if a glycinergic component, mediated by numerous small amplitude IPSCs under control conditions, were partially replaced by disinhibition of a tonic GABA component with fewer, large amplitude IPSCs.

L-AP4 caused a significant, 67 ± 5.5% decrease in the current noise (n = 12, $p < 0.05$, Figure 3.1 E), suggesting that much of the tonic inhibition is mediated via the ON pathway, which is consistent with the finding that L-AP4 blocked a fraction of the disinhibition, however these measurements did not reach significance (Fig. 3.1 A1). Consistent with the data above, NBQX produced a similar effect to L-AP4, supporting the contention that the ON-pathway inhibition is not mediated via ON bipolar cell gap-junctions with AII amacrine cells (Figure 3.1 E).

Finally, a fraction of the disinhibitory conductance during dark phases of the stimulus (Figure 3.1 A) appeared to be resistant to L-AP4 and NBQX. Since this component is mediated by OFF bipolar cells, it must involve serial inhibitory connections between amacrine cells (See circuit model in Figure 3.4). Such networks have recently been proposed for inhibition at bipolar cell terminals (Eggers and Lukasiewicz, 2010).

ON pathway-driven inhibition increases OFF BS RGC sensitivity to higher temporal frequencies

L-AP4 did not significantly affect the excitatory drive to OFF BS RGCs. Therefore we used L-AP4 to probe the role of crossover inhibition in generating the spiking properties at a range of contrasts and temporal frequencies. At a given contrast, blocking

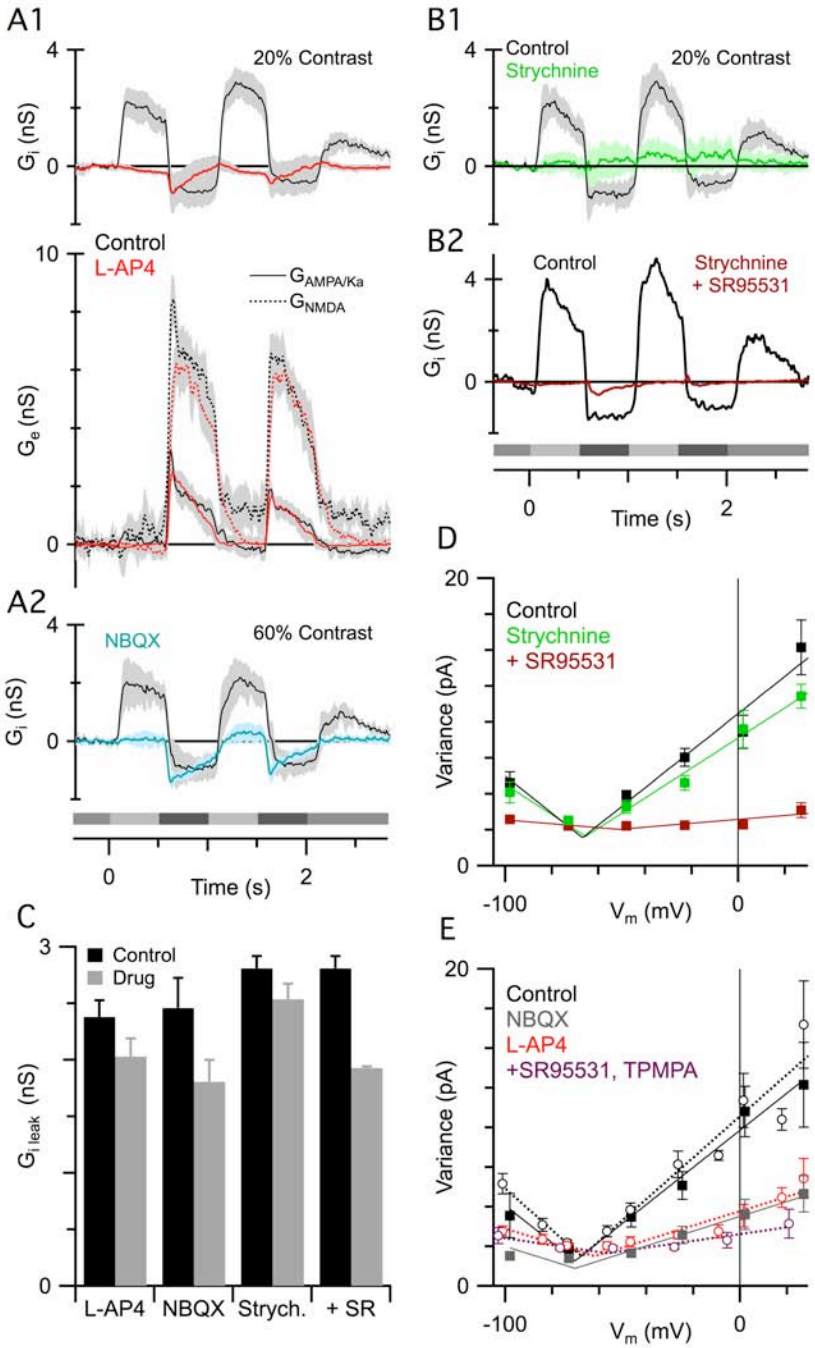

Figure 3.1. ON bipolar cells drive light-evoked inhibition in OFF BS RGCs via glycinergic amacrine cells, while OFF bipolar cells regulate a tonic GABAergic input.
A1, Mean inhibitory (top plot) and excitatory (NMDA and AMPA/KA bottom plot) light flash-evoked conductances derived from voltage-clamp recordings in 12 OFF BS RGCs with bath-applied 100 µM L-AP4 (red traces) and under control conditions (black traces). L-AP4 only affected inhibition.
A2, Mean inhibitory conductances as in A1. 25 µM NBQX in the bath (blue trace, n = 6 cells) and matched controls (black trace). NBQX has same affect as L-AP4 (A1).
B, Same as A2, but with blockers of inhibition.
B1 1 µM strychnine blocks most inhibition (n = 7 cells).
B2, Strychnine with 25 µM SR95531 in the bath (n=8).
C, Tonic inhibition measured by the effects of above drugs on the inhibitory component (current at E_{exc}) of the leak conductance. All drugs significantly decreased $G_{i\ leak}$ relative to control ($p < 0.05$). Strychnine caused the smallest decrease; significantly smaller than strychnine and SR combined (n=4; $p < 0.05$).
D, Mean variance of the current plotted against membrane voltage. Slope of linear fit indicates relative amplitude of tonic inhibitory input. Strychnine did not significantly reduce current variance (n = 7). Addition of SR reduced the tonic inhibitory input to baseline levels (n = 8).
E, Current variance plot as in D. NBQX (filled, n=6) and L-AP4 (open, n=12) suppressed a similar proportion of tonic inhibition. It was further reduced by SR and 50 µM TPMPA (n=4).

the ON-pathway with L-AP4 blocked progressively mores spikes as temporal frequency increased (Figure 3.2 A, B & C). The frequency-dependence arises because the effects of crossover inhibition appeared to be transient; blocking crossover inhibition had a significant effect on the spike rate during the initial 50 ms of the response at all frequencies (Figure 3.2 D). Moreover, the L-AP4 effects indicate that crossover inhibition, similar to the NMDA component of excitation, is more potent at low contrasts, at least when the analysis was restricted to the first stimulus cycle (Figure 3.2 C). Whole-cell voltage clamp recordings showed that for the first stimulus cycle the amplitude of inhibitory conductance showed a small increase from 2 to 8 Hz, while the amplitude of the AMPA/KA component decreased between these frequencies (Figures 3.2 E1 − 3 and 3.2 F). We further examined the dynamics of ON pathway contribution to OFF BS RGC spike output by presenting a dark spot that would preferentially drive the OFF pathway, or a bright spot that would drive the ON pathway. Due to the rectification of the OFF pathway (Figure 3.2 E), the OFF responses elicited by extinguishing the bright stimulus were about half that produced by the onset of the dark stimulus of the same amplitude (Figures 3.3 A1 and B1). Moreover, for the bright spot, the entire response within the first 50 ms was driven by the ON pathway input, since it was almost completely suppressed by L-AP4 (Figure 3.3 B1). In the 4 cells tested, L-AP4 attenuated the peak spike rate by 88%, and delayed the latency to the peak by 200 ms (Figure 3.3 B1). By contrast, L-AP4 had a much smaller effect on the response to the dark spot; a 29% attenuation of the peak spike rate, and only a 10 millisecond increase in latency to peak firing rate (Figure 3.3 A1). The timing of underlying conductances correlated well with the spiking. For the dark spot, in control, the onset of spiking in Figure 3.3 A1

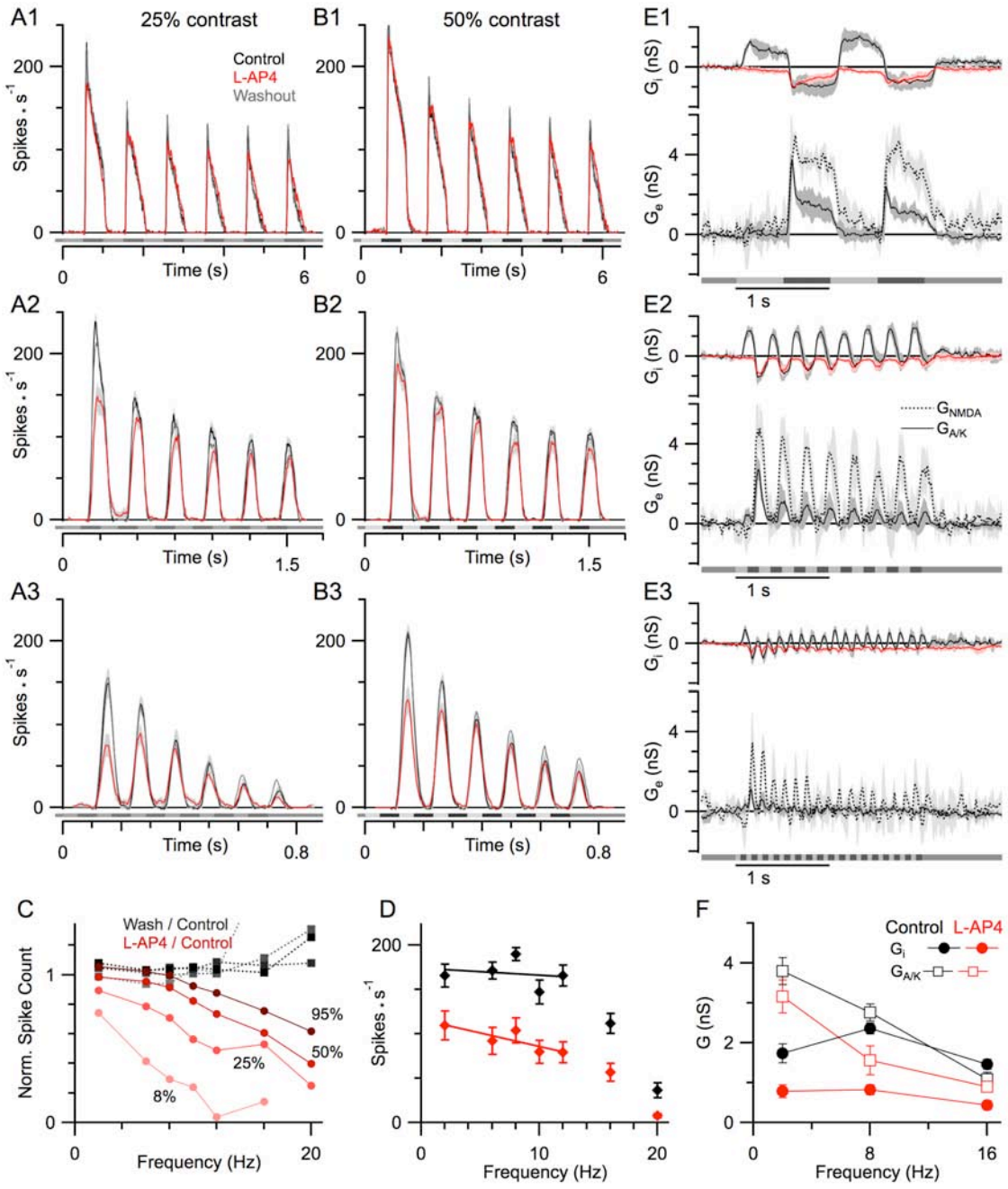

Figure 3.2. ON pathway-driven disinhibition contributes to the transient component of spike output in OFF BS RGCs, enhancing sensitivity to higher frequency stimuli.
A, Mean peristimulus spike time histograms (PSTH) of responses from 8 OFF BS RGCs to a focal spot stimulus of moderate contrast (25%), flicker frequencies: 2 Hz (A1), 8 Hz (A2) and ~ 16 Hz (A3). Control PSTHs are black, responses with bath applied 100 µM L-AP4 are red, and drug washout are grey traces. **B,** Same as A but at a saturating stimulus contrast (50%).
C, Mean number of spikes for the L-AP4 and washout conditions generated during the first response cycle in A and B, normalized to control. The shades of red represent the different stimulus contrasts; 8%, 25%, 50%, & 90%, lightest to darkest. Suppression of spiking for the two highest contrasts was observed only at the highest stimulus frequencies.
Figure caption continued on next page…

Figure 3.2 continued…
D, The mean firing rates during the transient phase, first 50 ms of the first cycle of each stimulus at 25% contrast, showing a greater suppression of spiking by L-AP4 at stimulus frequencies between 6 and 12 Hz. Under control conditions, the firing rate did not drop significantly between 2 and 12 Hz.
E, Mean plots of inhibitory and AMPA/KA components of membrane conductance for 2 Hz (F1), 8 Hz(F2) and ~16 Hz (F3) in 4 OFF BS RGCs.
F, Summary plot of conductance amplitudes for the first cycle of the light responses in F. The amplitude of the spike output under control conditions (D), varied similarly to the amplitude of G_i (F). G_i maintained its amplitude between 2 Hz (E1) and 8 Hz (E2), but decreased at 16 Hz. L-AP4 caused spiking to decrease monotonically with $G_{AMPA/KA}$, the excitatory component that makes the greatest contribution to spiking output.

Figure 3.3.
ON amacrine cell-driven inhibition expands OFF BS RGC dynamic range.

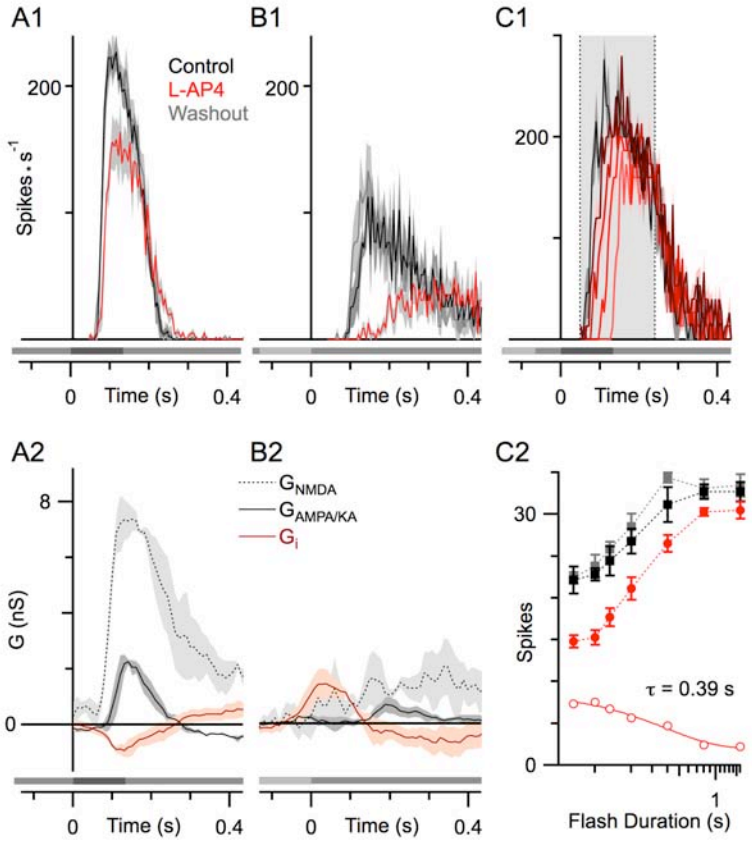

A1, Mean poststimulus spike time histograms of 4 OFF BS RGC responses to a 130 ms dark focal light step to 80% of background luminance. Bath application of 50 µM L-AP4 attenuated the response (red trace).
A2, Plots of mean excitatory and inhibitory membrane conductances from 3 OFF BS cells in response to the same stimulus.
B1 and 2, Same as A, except the stimulus was a bright light step 120% of background luminance. Decreasing inhibition in B2 corresponds to the rising phase of the control (black) PSTH in B1. The timing of $G_{AMPA/KA}$ increase in B2 corresponds to the rising phase of the L-AP4 (red) PSTH in B1.
C, Adaptation of ON pathway contribution to OFF BS RGC spike output.
C1, In the same cells as in A1 and B1, a dark 130 ms luminance step was preceded by a bright step lasting 800 ms under control conditions (black trace) and 100, 200, 400 or 800 ms in the presence of L-AP4 (traces in darkening shades of red).
C2, RGC spike output from C1 summarized as the mean number of spikes generated in the 300 ms (shaded area in C1) following the dark flash onset plotted against the preceding bright flash duration. The best fit for the difference in the spiking between control and drug conditions was provided by a single exponential decay function with a τ = 390 ms.

appeared to correlate well with the onset of excitation (Figure 3.3 A2), while for the bright spot, spiking onset under control conditions (Figure 3.3 B1) corresponded to a sharp decrease in inhibition in Figure 3.3 B2. For the bright spot, the presence of L-AP4 delayed and slowed the rise in spiking (red trace in Figure 3.3 B1), resulting in a response with time course similar to the delayed excitation (Figure 3.3 B2).

With the ON-pathway blocked, the peak response amplitude showed less contrast adaptation during consecutive stimulus cycles (see Fig. 3.2 A3, B3). We tested the time-course of this L-AP4 sensitive adaptation by flashing a bright spot for different durations and measuring the response to a subsequent dark spot with or without L-AP4 in the bath (Figure 3.3 C1). After an 800 ms flash, the ON pathway made no contribution to OFF BS RGC spiking, whereas progressively shorter flashes revealed an increasing ON-pathway contribution (Figures 3.3 C1 and 3.3 C2). The contribution of the ON pathway to spiking, as a function of flash duration, decayed with a time constant of 0.39 seconds. Considering that the inhibitory input did not show much adaptation during 500 ms light steps (Figure 3.1 A1 and 3.2 E2), the fast time-course of adaptation of ON pathway contribution to spiking is likely due to an intrinsic property of the RGC.

Discussion

The ON pathway contributes to high temporal frequency sensitivity via a novel amacrine cell pathway.

The primary light-evoked inhibitory input to OFF BS RGCs is via a glycinergic amacrine cell, which is driven by ON bipolar cells. During a flickering stimulus this input provides inhibition during the bright phase, and its shut-off during the dark phase contributes to excitation. At low flicker frequencies (< 6 Hz), blocking the ON pathway,

which drives this inhibition, does not affect the spike output even for low contrast stimuli. However, spiking is strongly attenuated at higher frequencies. Thus, this feed-forward inhibitory input appears to underlie much of the sensitivity of OFF BS RGC to high frequency stimuli.

ON pathway mediated crossover inhibition has been demonstrated in OFF α RGCs in the guinea pig and mouse, and provides the main excitatory drive at low contrasts (Manookin et al., 2008; van Wyk et al., 2009). Crossover inhibition in OFF α RGCs is mediated by direct AII glycinergic inputs, which are driven by connexin-36 gap-junction connections from ON bipolar cells. Thus, this crossover inhibition is not blocked by NBQX, and is absent in connexin-36 knockout animals (van Wyk et al., 2009). In contrast, crossover inhibition in OFF BS RGCs is blocked by NBQX, suggesting that, unlike the AII amacrine, it originates from an amacrine cell that receives conventional glutamatergic inputs from ON cone bipolar cells. There are several types of narrow-field glycinergic amacrine cells in the rabbit, which could mediate such a connection (MacNeil et al., 1999).

A key difference between OFF BS RGCs and α RGCs is in the mode of action of the crossover inhibition. A tonic glycinergic input from the AII amacrine cells to OFF α RGCs is essential to allow for the dis-inhibitory excitation during negative contrast stimuli. However, while OFF BS RGCs receive a tonic inhibitory input, it is only partially mediated by glycinergic crossover inhibition. More importantly, blocking the ON pathway did not have a substantial effect on disinhibition during the OFF-phase of the stimulus. Thus, suppression of tonic inhibition during decreases in light intensity cannot be used as a mechanism to explain how L-AP4 suppresses BS RGC spike output.

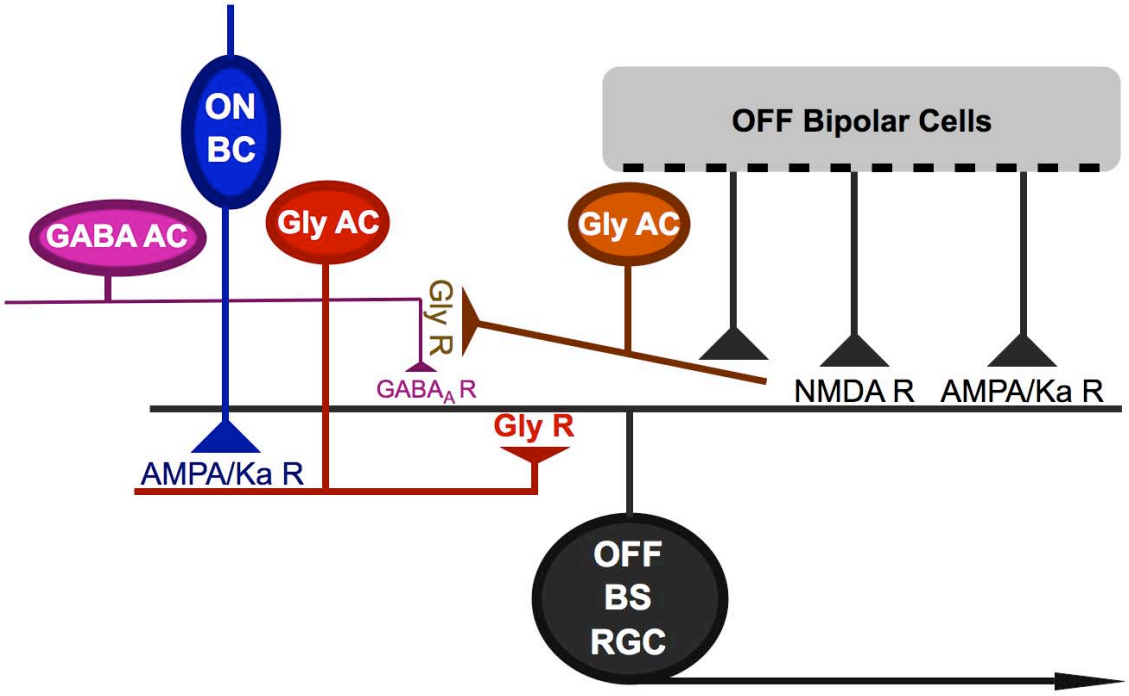

Figure 3.4 Glycinergic and GABAergic inputs to OFF BS RGCs.
The primary inhibitory input to OFF BS RGCs is glycinergic and provided by an amacrine cell that is driven by the ON channel via AMPA/KA receptors. OFF BS RGCs also receive a small, tonic GABAergic input, which is revealed when glycine receptors are blocked.

We therefore propose that the effects of cross-over inhibition in OFF BS RGCs are mediated through hyperpolarization during increases in light intensity rather than depolarization due to a decrease in a tonic inhibitory conductance as seen in OFF α RGCs. Hyperpolarization may prime BS RGCs to produce transient rebound excitation, perhaps driven by low voltage activated Ca^{2+} channels as has been demonstrated in other RGC types (Mitra and Miller, 2007; Margolis et al., 2010). This idea is supported by our observation that L-AP4 strongly attenuated spiking in response to the dimming of a bright flash, but had minimal effect to a similar negative contrast step, which produced

more spiking. Moreover, the transient nature of our proposed mechanism for the action of crossover inhibition correlates with its larger contribution to spike output observed at high frequencies. Since the excitatory inputs to OFF BS RGCs are strongly rectified, and respond very weakly to short bright flashes, we conclude that crossover inhibition is critical for maintaining BS RGC temporal sensitivity at both positive and negative contrasts.

The comparison between OFF α RGCs and OFF BS RGCs demonstrates that despite the similarities in receptors and connectivity the inputs appear to be utilized in different ways. OFF BS RGCs, defined by their tonic signalling, have crossover inhibition that acts transiently to enhance their sensitivity to high temporal frequencies. On the other hand, OFF α RGCs, perhaps the quintessential transient cells, are driven by decreases in a tonically active inhibition, which enhances their contrast sensitivity.

A novel facet of the crossover inhibition seen in OFF BS RGCs is its contribution to contrast adaptation, particularly at high frequencies. Hosoya and colleagues (2005) suggested that inputs from amacrine cells enhance RGC responses to novel stimuli, and subsequent adaptation. However, no specific circuit has been identified. We show that ON crossover inhibition contributes to contrast adaptation in OFF BS RGCs by enhancing responses to the first few stimulus cycles. In the absence of ON inhibition, OFF BS RGCs have a weaker response to an increase in temporal contrast, and hence weaker contrast adaptation.

Chapter 4

Conclusions and Follow-up Experiments.

NMDA receptors in visual processing.

The main finding of the first part of this work is that NMDA receptors contribute to temporal contrast encoding in OFF BS RGCs. They do so in a stimulus intensity-dependent way. Although NMDA inputs increase the gain of responses across the entire range of stimulus contrast, there is a heightened effect for very low contrasts at which the stimulus is encoded by a very small number of spikes. For a neuron with a low maintained firing rate, such as the OFF BS RGC, detection of a very small change in temporal contrast could depend on the presence of just a few action potentials. Thus, the inability to encode a weak stimulus in the absence of NMDA receptor signaling in the retina could have important behavioral repercussions.

Other researchers investigating the contribution of NMDA receptors to visual stimulus encoding in RGCs did not observe a specific low contrast effect of blocking NMDA receptors (Manookin et al., 2010). These investigators recorded from OFF α RGCs, which have large receptive fields and a very different dendritic morphology from the OFF BS RGCs described here. The other OFF type cell from which Manookin et al. recorded, the δ RGC (Margolis and Detwiler, 2007), only had an NMDA receptor contribution to spike output in response to high contrast stimuli. They also found that ON α RGCs lack a significant NMDA receptor contribution to spike output, in line with

evidence showing that ON RGCs lack synaptically-expressed NMDA receptors (Sagdullaev et al., 2006; Zhang and Diamond, 2009; Manookin et al., 2010). Along with the finding that LED RGCs, which get inputs from both ON and OFF bipolar cells, have a very linear IV, appearing to lack a significant light-evoked NMDA receptor input (van Wyk et al., 2006), this evidence suggests a very pathway-specific NMDA receptor contribution to visual stimulus encoding in the retina.

This raises the question: what specifically about OFF BS RGCs or their presynaptic circuitry makes them rely on NMDA receptors to encode weak stimuli? This question is particularly interesting in light of the accepted roles for NMDA receptors in the central nervous system. NMDA receptors are often thought to play a secondary role to AMPA and kainate receptors in signal transduction due to being blocked by Mg^{+2} at resting membrane potentials and requiring initial depolarization of the postsynaptic membrane by activation of cationic conductance through other glutamate receptors. The relatively high Ca^{2+} permeability of NMDA receptors also makes them ideal for initiating molecular signalling cascades, which depend on Ca^{2+} and affect gene expression and protein localization. This has led to a view of NMDA receptors as modulators of synaptic strength with a primary role in synaptic plasticity. A recent review by Kerchner and Nicoll (2008) details the role of synaptic NMDA receptors in long-term potentiation at central synapses. Likewise, developmental changes in NMDA receptor subunit composition, which affect their Ca^{2+} permeability, have implicated NMDA receptors as messengers in the development of synaptic circuitry (Hahm et al., 1991; Adesnik et al., 2008) However, as outlined in the introduction, recent evidence is pointing to more examples where NMDA receptors may play a direct role in signal transduction in sensory

and multimodal cortical neurons. This is particularly the case in the OFF pathway of the retina. However, a question remains as to how NMDA receptors there can directly contribute to spike generation.

Based on the conventional view, it should not be possible for NMDA receptors to generate responses to weak stimuli, such as seen in OFF BS RGCs, in the absence of prior AMPA receptor activation. I propose some experiments to address this issue. The first series of experiments would involve intracellular recordings from OFF BS RGCs in current clamp mode while isolating NMDA inputs using AMPA/KA and glycine receptor antagonists. OFF BS RGCs continue receiving glutamatergic inputs from OFF bipolar cells even in the presence of AMPA/KA receptor blockers such as NBQX or CNQX, as shown in Figure 2.5B. Thus, NMDA receptor inputs can be isolated by blocking AMPA receptors, and by blocking the primary light-evoked inhibitory input, which is glycinergic, with strychnine (Figure 3.1). These recordings would be done using sharp, potassium acetate electrodes in order to prevent washout of intracellular components that may be involved in NMDA receptor signaling and spike generation. Spike output in OFF BS RGCs was strongly reduced within several minutes of the start of recording when using low resistance patch electrodes (Data not shown). Although perforated patch recordings may be preferable in order to prevent disruption of intracellular components, they are very challenging to perform on somas of small RGCs in the whole-mount retina preparation due to the amount of intervening extracellular debris. Temporal contrast of the stimulus in these experiments would be varied from near the threshold for detection, approximately 3%, to saturating contrast, near 40%.

The expected outcome of this experiment, based on extracellular − loose-patch recordings and the results attained in voltage clamp mode, is that NMDA receptors alone would be able to depolarize the cell even at 3% contrast. Based on NMDA puffing experiments, a portion of NMDA receptors in OFF BS RGCs is expected to remain unblocked even at resting membrane potentials between -80 and -60 mV (Figure 1.2). Additionally, a study in primate OFF RGCs, showed that a small spiking response remained in the presence of AMPA/KA receptor antagonists, and that it was sensitive to D-AP7, an NMDA receptor antagonist (Cohen and Miller, 1994). Conductance through a portion of NMDA receptor channels may depolarize the cell if they are synaptically localized and are exposed to transiently high glutamate concentrations in response to focal light intensity decreases.

If low contrast stimuli do not depolarize the cell by activating NMDA receptors alone, then some amount of AMPA receptor activation may be required in order for NMDA receptors to depolarize the cell towards spike threshold, or cause a dendritic spike in order to trigger a somatic spike. This could be tested using the current-clamp recording method described above, except that NMDA receptors would be blocked by superfusion of the antagonist D-AP5. One outcome of this experiment would be that blocking NMDA receptors would reduce spiking and depolarization for low contrast stimuli.

Another hypothesis for NMDA receptor contribution to low stimulus contrast responses is that Ca^{2+} signaling through NMDA receptors could enhance dendritic spike initiation. NMDA receptors have been shown to affect intrinsic excitability of cerebellar deep nuclear neurons by lowering their spike initiation threshold (Aizenman and Linden, 2000), and in CA1 hippocampal neurons, NMDA receptors may contribute to intrinsic

excitability by lowering the activation threshold for voltage-gated sodium channels (Xu et al., 2005a). Although these potentiation effects produced by NMDA receptor activation have long time constants (tens of minutes) and are long-lasting, the extracellular recordings using NMDA receptor antagonists presented here in chapter 2 took many minutes to complete, and drug washout sometimes did not restore spiking to initial levels (Figure 2.5).

Some RGCs are known to generate dendritic spikes (Velte and Masland, 1999; Oesch et al., 2005). Dendritic spikes in direction-selective RGCs have been shown to evoke somatic action potentials (Oesch et al., 2005). Although it remains to be tested whether OFF BS RGCs also have active dendrites, I have observed small "spikelets" during extracellular recordings, so this is a possibility. An experiment to test the hypothesis that NMDA receptors contribute to electrical activity in OFF BS RGC dendrites would require revealing the dendritic spikes. Somatic spikes may be blocked by a local application of tetrodotoxin to the soma or by a low concentration of intracellular lidocaine HCl (Oesch et al., 2005).

If OFF BS RGCs indeed have dendritic spikes mediated by voltage-activated sodium channels as was the case in direction-selective RGCs (Oesch et al., 2005), it would be interesting to explore how they contribute to spatial summation. In an RGC, two spatially dissimilar stimuli can evoke a similar pattern of spiking. A low contrast spot, which illuminates the entire center the receptive field, similar to the stimuli used in the experiments described in the earlier chapters, may evoke a similar number of action potentials as a very small, but high contrast spot. It is unknown, whether such spatially distinct stimuli would also evoke a similar number of dendritic spikes. This is because a

large stimulus would presumably cause a weak depolarization over the entire dendritic field, whereas a focal stimulus might strongly depolarize a small patch of dendrites. Using the selective block of somatic action potentials, one could test whether two stimuli of the same cumulative intensity, but different spatial scale would differentially affect dendritic spiking. Similarly, it would be interesting to test whether NMDA receptors vary their contribution to RGC responses depending on the spatial scale of a stimulus. The results of this experiment could vary among different RGC types, as it has been shown that β RGCs have a higher density of synapses on their dendrites than α cells (Kier et al., 1995).

Finally, there is some evidence that NMDA receptor contribution to light-evoked responses in OFF BS RGCs could be presynaptic. Although blocking NMDA receptors had no effect on the linear, AMPA/KA, component of excitation (Figure 2.3), we observed a small reduction in the amount of disinhibition (~ 1 nS) that occurred in response to focal dark stimuli (Figure 4.1). The disinhibition is presumably a result of a stimulus-evoked decrease in a tonic inhibitory input from amacrine cells. It is unclear how blocking NMDA receptors would result in a reversal of this disinhibition, but if that is truly the case, the firing rate of the postsynaptic RGC could be affected. Responses to NMDA have been identified in a variety of amacrine cell types, mostly those with wide receptive fields and GABA synthesis (Kalloniatis et al., 2004; Dumitrescu et al., 2006). One way to test whether the contribution of NMDA receptors is via presynaptic circuitry, is to isolate NMDA receptors on amacrine cells by blocking only the postsynaptic NMDA receptors. This may be done by including open-channel blocker MK-801 in the recording pipette (Berretta and Jones, 1996; Manookin et al., 2010). Any additional

contribution of NMDA receptors arising from decreases in inhibition could then be selectively blocked with bath-applied D-AP5. This experiment would reveal whether NMDA receptors affect contrast sensitivity in the retinal OFF channel through their activity in amacrine cells.

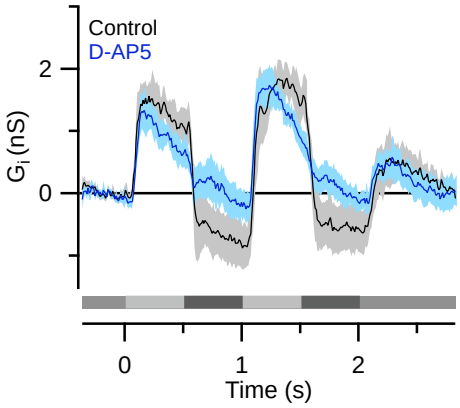

Figure 4.1 Blocking NMDA receptors affects light-evoked inhibition in OFF BS RGC. Mean inhibitory conductance evoked in 8 OFF BS RGCs by a 20% temporal contrast stimulus in the presence of bath applied 50 µM D-AP5 (blue trace), and control (black trace). Blocking NMDA receptors reduced the phasic disinhibition during the dark phase of the stimulus, but did not affect the bright phase-driven inhibition, which is caused by an ON channel crossover input (Figure 3.1).

NMDA receptors in the ON channel

NMDA receptors appear to play a different role in ON RGCs than they do in the OFF pathway. Recent studies show that NMDA receptors are mostly extrasynaptic in ON RGCs, have different subunit composition, and are activated by glutamate spillover (Sagdullaev et al., 2006; Grimes et al., 2010). Although they can be activated by agonist application, they may not contribute much to EPSCs, and are therefore not directly involved in signal transduction. Rather they may play a developmental or protein expression and localization regulatory role. Blocking NMDA receptors in ON α cells did

not result in a significant decrease in light-evoked spiking (Manookin et al., 2010). However, major differences in NMDA receptor expression and contribution have been reported among OFF RGCs, so it is possible that some ON cells, especially small ones, which have not been as extensively studied, also have synaptic NMDA receptors.

My recordings from ON BS RGCs showed the presence of an NMDA receptor component of light-evoked excitation, which was smaller than the NMDA component seen in OFF BS RGCs (Figure 4.2). Cohen (2000) has also reported a significant NMDA contribution to light-evoked excitation in cat ON X-type RGCs. It is worthwhile to consider whether NMDA receptors are involved in visual contrast encoding in the high acuity pathway, rather than just being limited to the OFF channel.

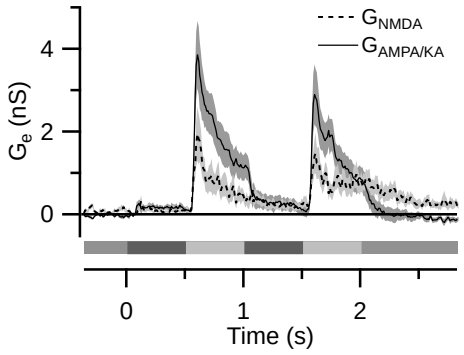

Figure 4.2 NMDA and AMPA/KA components of excitation in ON BS RGCs.
Mean NMDA and AMPA/KA receptor components of excitatory conductance derived from IV relations of 10 ON BS RGCs evoked by a 20% contrast flickering focal stimulus. The NMDA component is smaller than in OFF BS RGCs. Compare to conductance plots in Figure 2.2.

Crossover inhibition, a multimodal retinal circuit

The work described in chapter 3 contributes to the recent discovery that glycinergic amacrine cells mediate crosstalk between the ON and OFF channels of visual information processing (O'Brien et al., 2003; Zaghloul et al., 2003; Molnar and Werblin,

2007; Manookin et al., 2008; Molnar et al., 2009; Munch et al., 2009; van Wyk et al., 2009). We found that in OFF BS RGCs, crossover inhibition contributes to the transient component of spike generation and therefore increases contrast gain at higher temporal frequencies (Figure 3.2). The other major finding was that crossover inhibition contributes to contrast adaptation, disproportionately increasing the initial response to a quickly flickering spot, and driving most of the response to the dimming of briefly flashed bright spots (Figure 3.3). Thus, crossover inhibition would likely enhance the ability of the neuron to respond to a stimulus that had rapidly moved across the RGC receptive field, and reliably generate a response regardless of whether it was dark or bright.

Although ON-driven inhibition in OFF BS RGCs has a steep rising phase in response to light intensity increases, and is quickly shut off by dimming light stimuli, the input is not transient, and is maintained for the duration of a light step (Figure 4.1). This is in contrast to the transient inhibitory inputs attributed to crossover inhibition in mouse looming-detector RGCs (Munch et al., 2009), guinea pig α cells (Manookin et al., 2008), and the transient light responses recorded in AII amacrine cells (Bloomfield and Volgyi, 2004; Munch et al., 2009). Contrary to previous evidence that gap junctions mediate crossover inhibition, we found that crossover inhibition to OFF BS RGCs could be blocked by AMPA receptor antagonists, and is thus not likely to be transmitted via electrical coupling from the ON bipolar to AII amacrine cell. We therefore conclude that the crossover inhibition in OFF BS RGCs is mediated by a glycinergic amacrine cell other than the AII.

Aside from the AII, relatively little is known about light responses or connectivity of glycinergic amacrine cells (Kolb and Nelson, 1981; Kolb et al., 1981; Kolb and Nelson, 1996). Recently developed transgenic mice expressing fluorescent proteins driven by cell type-specific promoters would make it possible to distinguish between different types of amacrine cells types during physiological experiments (Dumitrescu et al., 2006; Cherry et al., 2009). Specifically, glutamate receptor expression was studied in a mouse line expressing enhanced green fluorescent protein (EGFP) under the control of the glycine transporter 2 (GlyT2) promoter (Zeilhofer et al., 2005; Dumitrescu et al., 2006). Even though glycinergic amacrine cells only express GlyT1 (Menger et al., 1998), in these transgenic mice, GlyT2-driven EGFP expression is mostly limited to glycinergic amacrine cells including the AII (Dumitrescu et al., 2006). Using two-photon excitation of EGFP at infrared wavelengths in order to prevent photoreceptor bleaching, fluorophore-expressing glycinergic cells can be targeted, and their light-responses recorded (Wei et al., 2010). During recordings, the cells would be filled with other fluorescent dyes or neurobiotin to further examine their dendritic morphology and gap-junctional coupling. Genetic markers for specific amacrine cell and ganglion cell types are just beginning to be identified, which opens up a future possibility of generating mouse lines expressing fluorescent proteins in small subsets of co-stratified ganglion and amacrine cells (Siegert et al., 2009). Ultimately this would make dual recordings of an amacrine and a ganglion cell an easier feat, and allow for a more direct way to study functional connectivity in the IPL.

In the meantime, RGCs in the rabbit retina remain a good platform for studying the integration and processing of signals from various retinal circuit elements. Crossover

inhibition, the focus of this work, has different temporal profiles and appears to play different roles in different types of OFF RGCs. In some RGCs, a large tonic inhibitory input is diminished by dimming stimuli, which equates to disinhibition (Manookin et al., 2008; van Wyk et al., 2009). In others, such as the OFF BS RGC, this input is rectified, not strongly active at baseline, and is only turned on in response to increases in light intensity (Munch et al., 2009). Here, in chapter 3, we showed that ON crossover inhibition contributes transient increases to light responses in OFF BS RGCs.

How can an input that only hyperpolarizes the cell also increase its activity? Low voltage-activated (LVA) Ca^{2+} currents have been identified in RGCs, and have been shown to evoke rebound spiking after hyperpolarizing voltage steps (Mitra and Miller, 2007; Margolis et al., 2010). As a follow-up I propose to test whether this mechanism is responsible for the contribution of crossover inhibition from the ON channel to OFF RGC responses. Recording in current-clamp mode, as described earlier for examining the NMDA receptor contribution, the experiment would involve both bright light flashes and hyperpolarizing current injections to test for presence of LVA Ca^{+2} currents. Potential LVA currents would be confirmed by their sensitivity to mibefradil (Pan et al., 2001; Mitra and Miller, 2007), or Ni^{2+} (Margolis et al., 2010). Next, the ON pathway would be blocked with L-AP4 to test whether the natural hyperpolarization induced by crossover inhibition is sufficient to induce LVA Ca^{2+} current activation, and a subsequent increase in rebound spiking. An additional proof of principle experiment would test whether the inactivation of LVA Ca^{2+} currents had a similar time constant as the adaptation of the crossover inhibition contribution to RGC responses shown in Figure 3.3.

If this hypothesis is borne out in OFF BS RGCs, it would be interesting whether the same mechanism extends to other types of OFF RGCs that receive crossover inhibition. RGCs with larger receptive fields that receive inputs from an array of amacrine cells could employ the adaptive properties of this input to encode changes of spatial distribution of stimuli within their receptive fields. Using disinhibition to boost spiking when a spatial change in contrast has occurred may allow RGCs to compute changes in orientation and motion of a stimulus as several recent studies have proposed (Smirnakis et al., 1997; Hosoya et al., 2005; Molnar et al., 2009). So depending on the type of RGC, the crossover input could play a very different computational role. Discerning the function of these circuits will remain an exciting challenge in future retinal research.

References

Adesnik, H, Li, G, During, MJ, Pleasure, SJ, Nicoll, RA (2008) NMDA receptors inhibit synapse unsilencing during brain development. Proc Natl Acad Sci U S A, 105:5597–5602.

Aizenman, CD, Linden, DJ (2000) Rapid, synaptically driven increases in the intrinsic excitability of cerebellar deep nuclear neurons. Nat Neurosci, 3:109–111.

Aizenman, E, Frosch, MP, Lipton, SA (1988) Responses mediated by excitatory amino acid receptors in solitary retinal ganglion cells from rat. J Physiol, 396:75–91.

Amthor, FR, Takahashi, ES, Oyster, CW (1989a) Morphologies of rabbit retinal ganglion cells with complex receptive fields. J Comp Neurol, 280:97–121.

Amthor, FR, Takahashi, ES, Oyster, CW (1989b) Morphologies of rabbit retinal ganglion cells with concentric receptive fields. J Comp Neurol, 280:72–96.

Ascher, P, Nowak, L (1988) The role of divalent cations in the N-methyl-D-aspartate responses of mouse central neurones in culture. J Physiol, 399:247–266.

Awatramani, GB, Slaughter, MM (2000) Origin of transient and sustained responses in ganglion cells of the retina. J Neurosci, 20:7087–7095.

BARLOW, HB (1953) Summation and inhibition in the frog's retina. J Physiol, 119:69–88.

BARLOW, HB, HILL, RM (1963) Selective sensitivity to direction of movement in ganglion cells of the rabbit retina. Science, 139:412–414.

Barlow, HB, Levick, WR (1965) The mechanism of directionally selective units in rabbit's retina. J Physiol, 178:477–504.

Baylor, DA, Fuortes, MG, O'Bryan, PM (1971) Receptive fields of cones in the retina of the turtle. J Physiol, 214:265–294.

Beaudoin, DL, Manookin, MB, Demb, JB (2008) Distinct expressions of contrast gain control in parallel synaptic pathways converging on a retinal ganglion cell. J Physiol, 586:5487–5502.

Berretta, N, Jones, RS (1996) Tonic facilitation of glutamate release by presynaptic N-methyl-D-aspartate autoreceptors in the entorhinal cortex. Neuroscience, 75:339–344.

Bloomfield, SA (1992) Relationship between receptive and dendritic field size of amacrine cells in the rabbit retina. J Neurophysiol, 68:711–725.

Bloomfield, SA, Dacheux, RF (2001) Rod vision: pathways and processing in the mammalian retina. Prog Retin Eye Res, 20:351–384.

Bloomfield, SA, Miller, RF (1986) A functional organization of ON and OFF pathways in the rabbit retina. J Neurosci, 6:1–13.

Bloomfield, SA, Volgyi, B (2004) Function and plasticity of homologous coupling between AII amacrine cells. Vision Res, 44:3297–3306.

Bloomfield, SA, Xin, D, Osborne, T (1997) Light-induced modulation of coupling between AII amacrine cells in the rabbit retina. Vis Neurosci, 14:565–576.

Borghuis, BG, Sterling, P, Smith, RG (2009) Loss of sensitivity in an analog neural circuit. J Neurosci, 29:3045–3058.

Boycott, BB, Wassle, H (1974) The morphological types of ganglion cells of the domestic cat's retina. J Physiol, 240:397–419.

Brandstatter, JH, Koulen, P, Wassle, H (1998) Diversity of glutamate receptors in the mammalian retina. Vision Res, 38:1385–1397.

Burkhardt, DA, Gottesman, J, Thoreson, WB (1988) Prolonged depolarization in turtle cones evoked by current injection and stimulation of the receptive field surround. J Physiol, 407:329–348.

Caldwell, JH, Daw, NW (1978) New properties of rabbit retinal ganglion cells. J Physiol, 276:257–276.

Chander, D, Chichilnisky, EJ (2001) Adaptation to temporal contrast in primate and salamander retina. J Neurosci, 21:9904–9916.

Chavez, AE, Diamond, JS (2008) Diverse mechanisms underlie glycinergic feedback transmission onto rod bipolar cells in rat retina. J Neurosci, 28:7919–7928.

Chen, L, Huang, LY (1992) Protein kinase C reduces Mg2+ block of NMDA-receptor channels as a mechanism of modulation. Nature, 356:521–523.

Chen, S, Diamond, JS (2002) Synaptically released glutamate activates extrasynaptic NMDA receptors on cells in the ganglion cell layer of rat retina. J Neurosci, 22:2165–2173.

Chen, X, Hsueh, HA, Greenberg, K, Werblin, FS (2010) Three forms of Spatial Temporal Feedforward Inhibition are Common to Different Ganglion Cell Types in Rabbit Retina. J Neurophysiol,

Cherry, TJ, Trimarchi, JM, Stadler, MB, Cepko, CL (2009) Development and diversification of retinal amacrine interneurons at single cell resolution. Proc Natl Acad Sci U S A, 106:9495–9500.

Chichilnisky, EJ, Kalmar, RS (2002) Functional asymmetries in ON and OFF ganglion cells of primate retina. J Neurosci, 22:2737–2747.

Cleland, BG, Dubin, MW, Levick, WR (1971) Sustained and transient neurones in the cat's retina and lateral geniculate nucleus. J Physiol, 217:473–496.

Cohen, E, Sterling, P (1986) Accumulation of (3H)glycine by cone bipolar neurons in the cat retina. J Comp Neurol, 250:1–7.

Cohen, E, Sterling, P (1990) Convergence and divergence of cones onto bipolar cells in the central area of cat retina. Philos Trans R Soc Lond B Biol Sci, 330:323–328.

Cohen, ED (1998) Interactions of inhibition and excitation in the light-evoked currents of X type retinal ganglion cells. J Neurophysiol, 80:2975–2990.

Cohen, ED (2000) Light-evoked excitatory synaptic currents of X-type retinal ganglion cells. J Neurophysiol, 83:3217–3229.

Cohen, ED, Miller, RF (1994) The role of NMDA and non-NMDA excitatory amino acid receptors in the functional organization of primate retinal ganglion cells. Vis Neurosci, 11:317–332.

Cohen, ED, Zhou, ZJ, Fain, GL (1994) Ligand-gated currents of alpha and beta ganglion cells in the cat retinal slice. J Neurophysiol, 72:1260–1269.

Coleman, PA, Miller, RF (1988) Do N-methyl-D-aspartate receptors mediate synaptic responses in the mudpuppy retina? J Neurosci, 8:4728–4733.

Cook, PB, McReynolds, JS (1998) Lateral inhibition in the inner retina is important for spatial tuning of ganglion cells. Nat Neurosci, 1:714–719.

Crook, JD, Peterson, BB, Packer, OS, Robinson, FR, Gamlin, PD, Troy, JB, Dacey, DM (2008a) The smooth monostratified ganglion cell: evidence for spatial diversity in the Y-cell pathway to the lateral geniculate nucleus and superior colliculus in the macaque monkey. J Neurosci, 28:12654–12671.

Crook, JD, Peterson, BB, Packer, OS, Robinson, FR, Troy, JB, Dacey, DM (2008b) Y-cell receptive field and collicular projection of parasol ganglion cells in macaque monkey retina. J Neurosci, 28:11277–11291.

Dacheux, RF, Miller, RF (1976) Photoreceptor-bipolar cell transmission in the perfused retina eyecup of the mudpuppy. Science, 191:963–964.

Dacheux, RF, Raviola, E (1986) The rod pathway in the rabbit retina: a depolarizing bipolar and amacrine cell. J Neurosci, 6:331–345.

Das, S, Sasaki, YF, Rothe, T, Premkumar, LS, Takasu, M, Crandall, JE, Dikkes, P, Conner, DA, Rayudu, PV, Cheung, W, Chen, HS, Lipton, SA, Nakanishi, N (1998) Increased NMDA current and spine density in mice lacking the NMDA receptor subunit NR3A. Nature, 393:377–381.

de Monasterio, FM (1978) Properties of concentrically organized X and Y ganglion cells of macaque retina. J Neurophysiol, 41:1394–1417.

Deans, MR, Volgyi, B, Goodenough, DA, Bloomfield, SA, Paul, DL (2002) Connexin36 is essential for transmission of rod-mediated visual signals in the mammalian retina. Neuron, 36:703–712.

Demb, JB, Sterling, P, Freed, MA (2004) How retinal ganglion cells prevent synaptic noise from reaching the spike output. J Neurophysiol, 92:2510–2519.

Demb, JB, Zaghloul, K, Haarsma, L, Sterling, P (2001a) Bipolar cells contribute to nonlinear spatial summation in the brisk-transient (Y) ganglion cell in mammalian retina. J Neurosci, 21:7447–7454.

Demb, JB, Zaghloul, K, Sterling, P (2001b) Cellular basis for the response to second-order motion cues in Y retinal ganglion cells. Neuron, 32:711–721.

DeVries, SH (2000) Bipolar cells use kainate and AMPA receptors to filter visual information into separate channels. Neuron, 28:847–856.

Devries, SH, Baylor, DA (1997) Mosaic arrangement of ganglion cell receptive fields in rabbit retina. J Neurophysiol, 78:2048–2060.

Diamond, JS, Copenhagen, DR (1993) The contribution of NMDA and non-NMDA receptors to the light-evoked input-output characteristics of retinal ganglion cells. Neuron, 11:725–738.

Dumitrescu, ON, Protti, DA, Majumdar, S, Zeilhofer, HU, Wassle, H (2006) Ionotropic glutamate receptors of amacrine cells of the mouse retina. Vis Neurosci, 23:79–90.

Eggers, ED, Lukasiewicz, PD (2006) GABA(A), GABA(C) and glycine receptor-mediated inhibition differentially affects light-evoked signalling from mouse retinal rod bipolar cells. J Physiol, 572:215–225.

Eggers, ED, Lukasiewicz, PD (2010) Interneuron circuits tune inhibition in retinal bipolar cells. J Neurophysiol, 103:25–37.

Enroth-Cugell, C, Robson, JG (1966) The contrast sensitivity of retinal ganglion cells of the cat. J Physiol, 187:517–552.

Euler, T, Detwiler, PB, Denk, W (2002) Directionally selective calcium signals in dendrites of starburst amacrine cells. Nature, 418:845–852.

Euler, T, Masland, RH (2000) Light-evoked responses of bipolar cells in a mammalian retina. J Neurophysiol, 83:1817–1829.

Famiglietti, EV (2004) Class I and class II ganglion cells of rabbit retina: a structural basis for X and Y (brisk) cells. J Comp Neurol, 478:323–346.

Famiglietti, EV (2005) "Small-tufted" ganglion cells and two visual systems for the detection of object motion in rabbit retina. Vis Neurosci, 22:509–534.

Famiglietti, EVJ, Kolb, H (1976) Structural basis for ON-and OFF-center responses in retinal ganglion cells. Science, 194:193–195.

Flores-Herr, N, Protti, DA, Wassle, H (2001) Synaptic currents generating the inhibitory surround of ganglion cells in the mammalian retina. J Neurosci, 21:4852–4863.

Fried, SI, Munch, TA, Werblin, FS (2002) Mechanisms and circuitry underlying directional selectivity in the retina. Nature, 420:411–414.

Gil, Z, Amitai, Y (1996) Adult thalamocortical transmission involves both NMDA and non-NMDA receptors. J Neurophysiol, 76:2547–2554.

Grimes, WN, Zhang, J, Graydon, CW, Kachar, B, Diamond, JS (2010) Retinal parallel processors: more than 100 independent microcircuits operate within a single interneuron. Neuron, 65:873–885.

Grunder, T, Kohler, K, Kaletta, A, Guenther, E (2000) The distribution and developmental regulation of NMDA receptor subunit proteins in the outer and inner retina of the rat. J Neurobiol, 44:333–342.

Hahm, JO, Langdon, RB, Sur, M (1991) Disruption of retinogeniculate afferent segregation by antagonists to NMDA receptors. Nature, 351:568–570.

Hampson, EC, Vaney, DI, Weiler, R (1992) Dopaminergic modulation of gap junction permeability between amacrine cells in mammalian retina. J Neurosci, 12:4911–4922.

Hartline, HK (1938) THE RESPONSE OF SINGLE OPTIC NERVE FIBERS OF THE VERTEBRATE EYE TO ILLUMINATION OF THE RETINA. Am J Physiol, 121:400–415.

Hochstein, S, Shapley, RM (1976a) Linear and nonlinear spatial subunits in Y cat retinal ganglion cells. J Physiol, 262:265–284.

Hochstein, S, Shapley, RM (1976b) Quantitative analysis of retinal ganglion cell classifications. J Physiol, 262:237–264.

Hosoya, T, Baccus, SA, Meister, M (2005) Dynamic predictive coding by the retina. Nature, 436:71–77.

HUBEL, DH, WIESEL, TN (1960) Receptive fields of optic nerve fibres in the spider monkey. J Physiol, 154:572–580.

Hull, C, Isaacson, JS, Scanziani, M (2009) Postsynaptic mechanisms govern the differential excitation of cortical neurons by thalamic inputs. J Neurosci, 29:9127–9136.

Ichinose, T, Lukasiewicz, PD (2005) Inner and outer retinal pathways both contribute to surround inhibition of salamander ganglion cells. J Physiol, 565:517–535.

Johnson, JW, Ascher, P (1990) Voltage-dependent block by intracellular Mg2+ of N-methyl-D-aspartate-activated channels. Biophys J, 57:1085–1090.

Kalbaugh, TL, Zhang, J, Diamond, JS (2009) Coagonist release modulates NMDA receptor subtype contributions at synaptic inputs to retinal ganglion cells. J Neurosci, 29:1469–1479.

Kalloniatis, M, Sun, D, Foster, L, Haverkamp, S, Wassle, H (2004) Localization of NMDA receptor subunits and mapping NMDA drive within the mammalian retina. Vis Neurosci, 21:587–597.

Kaneko, A (1970) Physiological and morphological identification of horizontal, bipolar and amacrine cells in goldfish retina. J Physiol, 207:623–633.

Kaneko, A (1971) Electrical connexions between horizontal cells in the dogfish retina. J Physiol, 213:95–105.

Kaplan, E, Shapley, RM (1982) X and Y cells in the lateral geniculate nucleus of macaque monkeys. J Physiol, 330:125–143.

Kay, CD, Ikeda, H (1989) The quinoxalinediones antagonise the visual firing of sustained retinal ganglion cells. Eur J Pharmacol, 164:381–384.

Kerchner, GA, Nicoll, RA (2008) Silent synapses and the emergence of a postsynaptic mechanism for LTP. Nat Rev Neurosci, 9:813–825.

Kier, CK, Buchsbaum, G, Sterling, P (1995) How retinal microcircuits scale for ganglion cells of different size. J Neurosci, 15:7673–7683.

Kim, KJ, Rieke, F (2001) Temporal contrast adaptation in the input and output signals of salamander retinal ganglion cells. J Neurosci, 21:287–299.

Koike, C, Obara, T, Uriu, Y, Numata, T, Sanuki, R, Miyata, K, Koyasu, T, Ueno, S, Funabiki, K, Tani, A, Ueda, H, Kondo, M, Mori, Y, Tachibana, M, Furukawa, T (2010) TRPM1 is a component of the retinal ON bipolar cell transduction channel in the mGluR6 cascade. Proc Natl Acad Sci U S A, 107:332–337.

Kolb, H, Famiglietti, EV (1974) Rod and cone pathways in the inner plexiform layer of cat retina. Science, 186:47–49.

Kolb, H, Nelson, R (1981) Amacrine cells of the cat retina. Vision Res, 21:1625–1633.

Kolb, H, Nelson, R (1996) Hyperpolarizing, small-field, amacrine cells in cone pathways of cat retina. J Comp Neurol, 371:415–436.

Kolb, H, Nelson, R, Mariani, A (1981) Amacrine cells, bipolar cells and ganglion cells of the cat retina: a Golgi study. Vision Res, 21:1081–1114.

KUFFLER, SW (1953) Discharge patterns and functional organization of mammalian retina. J Neurophysiol, 16:37–68.

Levick, WR (1967) Receptive fields and trigger features of ganglion cells in the visual streak of the rabbits retina. J Physiol, 188:285–307.

Liang, Z, Freed, MA (2010) The ON pathway rectifies the OFF pathway of the mammalian retina. J Neurosci, 30:5533–5543.

Linsenmeier, RA, Frishman, LJ, Jakiela, HG, Enroth-Cugell, C (1982) Receptive field properties of x and y cells in the cat retina derived from contrast sensitivity measurements. Vision Res, 22:1173–1183.

Lukasiewicz, PD (2005) Synaptic mechanisms that shape visual signaling at the inner retina. Prog Brain Res, 147:205–218.

Lukasiewicz, PD, McReynolds, JS (1985) Synaptic transmission at N-methyl-D-aspartate receptors in the proximal retina of the mudpuppy. J Physiol, 367:99–115.

MacNeil, MA, Heussy, JK, Dacheux, RF, Raviola, E, Masland, RH (1999) The shapes and numbers of amacrine cells: matching of photofilled with Golgi-stained cells in the rabbit retina and comparison with other mammalian species. J Comp Neurol, 413:305–326.

MacNeil, MA, Heussy, JK, Dacheux, RF, Raviola, E, Masland, RH (2004) The population of bipolar cells in the rabbit retina. J Comp Neurol, 472:73–86.

Manookin, MB, Beaudoin, DL, Ernst, ZR, Flagel, LJ, Demb, JB (2008) Disinhibition combines with excitation to extend the operating range of the OFF visual pathway in daylight. J Neurosci, 28:4136–4150.

Manookin, MB, Weick, M, Stafford, BK, Demb, JB (2010) NMDA receptor contributions to visual contrast coding. Neuron, 67:280–293.

Margolis, DJ, Detwiler, PB (2007) Different mechanisms generate maintained activity in ON and OFF retinal ganglion cells. J Neurosci, 27:5994–6005.

Margolis, DJ, Gartland, AJ, Euler, T, Detwiler, PB (2010) Dendritic calcium signaling in ON and OFF mouse retinal ganglion cells. J Neurosci, 30:7127–7138.

Massey, SC, Miller, RF (1990) N-methyl-D-aspartate receptors of ganglion cells in rabbit retina. J Neurophysiol, 63:16–30.

Masu, M, Iwakabe, H, Tagawa, Y, Miyoshi, T, Yamashita, M, Fukuda, Y, Sasaki, H, Hiroi, K, Nakamura, Y, Shigemoto, R, et, a (1995) Specific deficit of the ON response in visual transmission by targeted disruption of the mGluR6 gene. Cell, 80:757–765.

Matsui, K, Hosoi, N, Tachibana, M (1998) Excitatory synaptic transmission in the inner retina: paired recordings of bipolar cells and neurons of the ganglion cell layer. J Neurosci, 18:4500–4510.

Mayer, ML, Westbrook, GL (1985) The action of N-methyl-D-aspartic acid on mouse spinal neurones in culture. J Physiol, 361:65–90.

Mayer, ML, Westbrook, GL, Guthrie, PB (1984) Voltage-dependent block by Mg2+ of NMDA responses in spinal cord neurones. Nature, 309:261–263.

McGuire, BA, Stevens, JK, Sterling, P (1984) Microcircuitry of bipolar cells in cat retina. J Neurosci, 4:2920–2938.

McMahon, MJ, Packer, OS, Dacey, DM (2004) The classical receptive field surround of primate parasol ganglion cells is mediated primarily by a non-GABAergic pathway. J Neurosci, 24:3736–3745.

Menger, N, Pow, DV, Wassle, H (1998) Glycinergic amacrine cells of the rat retina. J Comp Neurol, 401:34–46.

Merwine, DK, Amthor, FR, Grzywacz, NM (1995) Interaction between center and surround in rabbit retinal ganglion cells. J Neurophysiol, 73:1547–1567.

Miller, KD, Chapman, B, Stryker, MP (1989) Visual responses in adult cat visual cortex depend on N-methyl-D-aspartate receptors. Proc Natl Acad Sci U S A, 86:5183–5187.

Mills, SL, Massey, SC (1995) Differential properties of two gap junctional pathways made by AII amacrine cells. Nature, 377:734–737.

Mitra, P, Miller, RF (2007) Mechanism underlying rebound excitation in retinal ganglion cells. Vis Neurosci, 24:709–731.

Mittman, S, Taylor, WR, Copenhagen, DR (1990) Concomitant activation of two types of glutamate receptor mediates excitation of salamander retinal ganglion cells. J Physiol, 428:175–197.

Molnar, A, Hsueh, HA, Roska, B, Werblin, FS (2009) Crossover inhibition in the retina: circuitry that compensates for nonlinear rectifying synaptic transmission. J Comput Neurosci, 27:569–590.

Molnar, A, Werblin, F (2007) Inhibitory feedback shapes bipolar cell responses in the rabbit retina. J Neurophysiol, 98:3423–3435.

Monyer, H, Burnashev, N, Laurie, DJ, Sakmann, B, Seeburg, PH (1994) Developmental and regional expression in the rat brain and functional properties of four NMDA receptors. Neuron, 12:529–540.

Morgans, CW, Zhang, J, Jeffrey, BG, Nelson, SM, Burke, NS, Duvoisin, RM, Brown, RL (2009) TRPM1 is required for the depolarizing light response in retinal ON-bipolar cells. Proc Natl Acad Sci U S A, 106:19174–19178.

Muller, F, Wassle, H, Voigt, T (1988) Pharmacological modulation of the rod pathway in the cat retina. J Neurophysiol, 59:1657–1672.

Munch, TA, da Silveira, RA, Siegert, S, Viney, TJ, Awatramani, GB, Roska, B (2009) Approach sensitivity in the retina processed by a multifunctional neural circuit. Nat Neurosci, 12:1308–1316.

Nakatani, K, Tamura, T, Yau, KW (1991) Light adaptation in retinal rods of the rabbit and two other nonprimate mammals. J Gen Physiol, 97:413–435.

Nawy, S, Jahr, CE (1990) Suppression by glutamate of cGMP-activated conductance in retinal bipolar cells. Nature, 346:269–271.

Nelson, R, Kolb, H (1983) Synaptic patterns and response properties of bipolar and ganglion cells in the cat retina. Vision Res, 23:1183–1195.

Nelson, R, Kolb, H (1985) A17: a broad-field amacrine cell in the rod system of the cat retina. J Neurophysiol, 54:592–614.

Nelson, R, Kolb, H, Freed, MA (1993) OFF-alpha and OFF-beta ganglion cells in cat retina. I: Intracellular electrophysiology and HRP stains. J Comp Neurol, 329:68–84.

Nowak, L, Bregestovski, P, Ascher, P, Herbet, A, Prochiantz, A (1984) Magnesium gates glutamate-activated channels in mouse central neurones. Nature, 307:462–465.

O'Brien, BJ, Richardson, RC, Berson, DM (2003) Inhibitory network properties shaping the light evoked responses of cat alpha retinal ganglion cells. Vis Neurosci, 20:351–361.

Oesch, N, Euler, T, Taylor, WR (2005) Direction-selective dendritic action potentials in rabbit retina. Neuron, 47:739–750.

Pan, ZH, Hu, HJ, Perring, P, Andrade, R (2001) T-type Ca(2+) channels mediate neurotransmitter release in retinal bipolar cells. Neuron, 32:89–98.

Pang, JJ, Abd-El-Barr, MM, Gao, F, Bramblett, DE, Paul, DL, Wu, SM (2007) Relative contributions of rod and cone bipolar cell inputs to AII amacrine cell light responses in the mouse retina. J Physiol, 580:397–410.

Pang, JJ, Gao, F, Wu, SM (2003) Light-evoked excitatory and inhibitory synaptic inputs to ON and OFF alpha ganglion cells in the mouse retina. J Neurosci, 23:6063–6073.

Peichl, L, Wassle, H (1979) Size, scatter and coverage of ganglion cell receptive field centres in the cat retina. J Physiol, 291:117–141.

Pu, ML, Amthor, FR (1990) Dendritic morphologies of retinal ganglion cells projecting to the lateral geniculate nucleus in the rabbit. J Comp Neurol, 302:675–693.

Raviola, E, Dacheux, RF (1987) Excitatory dyad synapse in rabbit retina. Proc Natl Acad Sci U S A, 84:7324–7328.

Rockhill, RL, Daly, FJ, MacNeil, MA, Brown, SP, Masland, RH (2002) The diversity of ganglion cells in a mammalian retina. J Neurosci, 22:3831–3843.

Roska, B, Molnar, A, Werblin, FS (2006) Parallel processing in retinal ganglion cells: how integration of space-time patterns of excitation and inhibition form the spiking output. J Neurophysiol, 95:3810–3822.

Roska, B, Werblin, F (2001) Vertical interactions across ten parallel, stacked representations in the mammalian retina. Nature, 410:583–587.

Russell, TL, Werblin, FS (2010) Retinal synaptic pathways underlying the response of the rabbit local edge detector. J Neurophysiol, 103:2757–2769.

Sagdullaev, BT, McCall, MA, Lukasiewicz, PD (2006) Presynaptic inhibition modulates spillover, creating distinct dynamic response ranges of sensory output. Neuron, 50:923–935.

Saito, T, Kaneko, A (1983) Ionic mechanisms underlying the responses of off-center bipolar cells in the carp retina. I. Studies on responses evoked by light. J Gen Physiol, 81:589–601.

Shapley, R, Hochstein, S (1975) Visual spatial summation in two classes of geniculate cells. Nature, 256:411–413.

Shapley, RM, Victor, JD (1978) The effect of contrast on the transfer properties of cat retinal ganglion cells. J Physiol, 285:275–298.

Siegert, S, Scherf, BG, Del Punta, K, Didkovsky, N, Heintz, N, Roska, B (2009) Genetic address book for retinal cell types. Nat Neurosci, 12:1197–1204.

Sivyer, B, Taylor, WR, Vaney, DI (2010) Uniformity detector retinal ganglion cells fire complex spikes and receive only light-evoked inhibition. Proc Natl Acad Sci U S A, 107:5628–5633.

Slaughter, MM, Miller, RF (1981) 2-amino-4-phosphonobutyric acid: a new pharmacological tool for retina research. Science, 211:182–185.

Slaughter, MM, Miller, RF (1983a) The role of excitatory amino acid transmitters in the mudpuppy retina: an analysis with kainic acid and N-methyl aspartate. J Neurosci, 3:1701–1711.

Slaughter, MM, Miller, RF (1983b) An excitatory amino acid antagonist blocks cone input to sign-conserving second-order retinal neurons. Science, 219:1230–1232.

Smirnakis, SM, Berry, MJ, Warland, DK, Bialek, W, Meister, M (1997) Adaptation of retinal processing to image contrast and spatial scale. Nature, 386:69–73.

Srinivas, M, Hopperstad, MG, Spray, DC (2001) Quinine blocks specific gap junction channel subtypes. Proc Natl Acad Sci U S A, 98:10942–10947.

Srinivasan, MV, Laughlin, SB, Dubs, A (1982) Predictive coding: a fresh view of inhibition in the retina. Proc R Soc Lond B Biol Sci, 216:427–459.

Sterling, P, Freed, MA, Smith, RG (1988) Architecture of rod and cone circuits to the on-beta ganglion cell. J Neurosci, 8:623–642.

Strettoi, E, Raviola, E, Dacheux, RF (1992) Synaptic connections of the narrow-field, bistratified rod amacrine cell (AII) in the rabbit retina. J Comp Neurol, 325:152–168.

Sucher, NJ, Kohler, K, Tenneti, L, Wong, HK, Grunder, T, Fauser, S, Wheeler-Schilling, T, Nakanishi, N, Lipton, SA, Guenther, E (2003) N-methyl-D-aspartate receptor subunit NR3A in the retina: developmental expression, cellular localization, and functional aspects. Invest Ophthalmol Vis Sci, 44:4451–4456.

Taylor, WR (1999) TTX attenuates surround inhibition in rabbit retinal ganglion cells. Vis Neurosci, 16:285–290.

Taylor, WR, Chen, E, Copenhagen, DR (1995) Characterization of spontaneous excitatory synaptic currents in salamander retinal ganglion cells. J Physiol, 486:207–221.

Taylor, WR, Vaney, DI (2002) Diverse synaptic mechanisms generate direction selectivity in the rabbit retina. J Neurosci, 22:7712–7720.

Thibos, LN, Werblin, FS (1978) The response properties of the steady antagonistic surround in the mudpuppy retina. J Physiol, 278:79–99.

Troy, JB (1983) Spatial contrast sensitivities of X and Y type neurones in the cat's dorsal lateral geniculate nucleus. J Physiol, 344:399–417.

van Wyk, M, Taylor, WR, Vaney, DI (2006) Local edge detectors: a substrate for fine spatial vision at low temporal frequencies in rabbit retina. J Neurosci, 26:13250–13263.

van Wyk, M, Wassle, H, Taylor, WR (2009) Receptive field properties of ON- and OFF-ganglion cells in the mouse retina. Vis Neurosci, 26:297–308.

Vaney, DI (1986) Morphological identification of serotonin-accumulating neurons in the living retina. Science, 233:444–446.

Vaney, DI, Gynther, IC, Young, HM (1991) Rod-signal interneurons in the rabbit retina: 2. AII amacrine cells. J Comp Neurol, 310:154–169.

Vaney, DI, Levick, WR, Thibos, LN (1981a) Rabbit retinal ganglion cells. Receptive field classification and axonal conduction properties. Exp Brain Res, 44:27–33.

Vaney, DI, Peichi, L, Boycott, BB (1981b) Matching populations of amacrine cells in the inner nuclear and ganglion cell layers of the rabbit retina. J Comp Neurol, 199:373–391.

Velte, TJ, Masland, RH (1999) Action potentials in the dendrites of retinal ganglion cells. J Neurophysiol, 81:1412–1417.

Veruki, ML, Hartveit, E (2002) Electrical synapses mediate signal transmission in the rod pathway of the mammalian retina. J Neurosci, 22:10558–10566.

Veruki, ML, Hartveit, E (2009) Meclofenamic acid blocks electrical synapses of retinal AII amacrine and on-cone bipolar cells. J Neurophysiol, 101:2339–2347.

Victor, JD (1987) The dynamics of the cat retinal X cell centre. J Physiol, 386:219–246.

Victor, JD, Shapley, RM, Knight, BW (1977) Nonlinear analysis of cat retinal ganglion cells in the frequency domain. Proc Natl Acad Sci U S A, 74:3068–3072.

Wassle, H (2004) Parallel processing in the mammalian retina. Nat Rev Neurosci, 5:747–757.

Wassle, H, Grunert, U, Rohrenbeck, J, Boycott, BB (1989) Cortical magnification factor and the ganglion cell density of the primate retina. Nature, 341:643–646.

Wassle, H, Puller, C, Muller, F, Haverkamp, S (2009) Cone contacts, mosaics, and territories of bipolar cells in the mouse retina. J Neurosci, 29:106–117.

Wassle, H, Schafer-Trenkler, I, Voigt, T (1986) Analysis of a glycinergic inhibitory pathway in the cat retina. J Neurosci, 6:594–604.

Wei, W, Elstrott, J, Feller, MB (2010) Two-photon targeted recording of GFP-expressing neurons for light responses and live-cell imaging in the mouse retina. Nat Protoc, 5:1347–1352.

Werblin, FS, Dowling, JE (1969) Organization of the retina of the mudpuppy, Necturus maculosus. II. Intracellular recording. J Neurophysiol, 32:339–355.

Wong, HK, Liu, XB, Matos, MF, Chan, SF, Perez-Otano, I, Boysen, M, Cui, J, Nakanishi, N, Trimmer, JS, Jones, EG, Lipton, SA, Sucher, NJ (2002) Temporal and regional expression of NMDA receptor subunit NR3A in the mammalian brain. J Comp Neurol, 450:303–317.

Xia, XB, Mills, SL (2004) Gap junctional regulatory mechanisms in the AII amacrine cell of the rabbit retina. Vis Neurosci, 21:791–805.

Xin, D, Bloomfield, SA (1997) Tracer coupling pattern of amacrine and ganglion cells in the rabbit retina. J Comp Neurol, 383:512–528.

Xin, D, Bloomfield, SA (1999) Comparison of the responses of AII amacrine cells in the dark- and light-adapted rabbit retina. Vis Neurosci, 16:653–665.

Xu, J, Kang, N, Jiang, L, Nedergaard, M, Kang, J (2005a) Activity-dependent long-term potentiation of intrinsic excitability in hippocampal CA1 pyramidal neurons. J Neurosci, 25:1750–1760.

Xu, Y, Dhingra, NK, Smith, RG, Sterling, P (2005b) Sluggish and brisk ganglion cells detect contrast with similar sensitivity. J Neurophysiol, 93:2388–2395.

Young, HM, Vaney, DI (1990) The retinae of Prototherian mammals possess neuronal types that are characteristic of non-mammalian retinae. Vis Neurosci, 5:61–66.

Yu, W, Miller, RF (1996) The mechanism by which NBQX enhances NMDA currents in retinal ganglion cells. Brain Res, 709:184–196.

Zaghloul, KA, Boahen, K, Demb, JB (2003) Different circuits for ON and OFF retinal ganglion cells cause different contrast sensitivities. J Neurosci, 23:2645–2654.

Zeilhofer, HU, Studler, B, Arabadzisz, D, Schweizer, C, Ahmadi, S, Layh, B, Bosl, MR, Fritschy, JM (2005) Glycinergic neurons expressing enhanced green fluorescent protein in bacterial artificial chromosome transgenic mice. J Comp Neurol, 482:123–141.

Zhang, AJ, Wu, SM (2009) Receptive fields of retinal bipolar cells are mediated by heterogeneous synaptic circuitry. J Neurosci, 29:789–797.

Zhang, J, Diamond, JS (2006) Distinct perisynaptic and synaptic localization of NMDA and AMPA receptors on ganglion cells in rat retina. J Comp Neurol, 498:810–820.

Zhang, J, Diamond, JS (2009) Subunit- and pathway-specific localization of NMDA receptors and scaffolding proteins at ganglion cell synapses in rat retina. J Neurosci, 29:4274–4286.

Zhou, ZJ, Marshak, DW, Fain, GL (1994) Amino acid receptors of midget and parasol ganglion cells in primate retina. Proc Natl Acad Sci U S A, 91:4907–4911.